The Optical and Ultraviolet Emission-Line Properties of Bright Quasars with Detailed Spectral Energy Distributions

Baitian Tang,[1,2,3] Zhaohui Shang,[1,4] Qiusheng Gu,[2] Michael S. Brotherton,[4] Jessie C. Runnoe,[4]

ABSTRACT

We present measurements and statistical properties of the optical and ultraviolet emission lines present in the spectra of 85 bright quasars which have detailed spectral energy distributions. This heterogeneous sample has redshifts up to $z = 1.5$ and is comprised of three subsamples that may be of particular utility: ultraviolet excess Palomar-Green quasars, quasars with far-ultraviolet coverage from FUSE, and radio-loud quasars selected to have similar extended radio luminosity originally selected for orientation studies. Most of the objects have quasi-simultaneous optical-ultraviolet spectra, with significant coverage in the radio-to-X-ray wavebands. The parameters of all strong emission lines are measured by detailed spectral fitting. Many significant correlations previously found among quasar emission-line properties are also present in this sample, e.g., the Baldwin effect, the optical correlations collectively known as eigenvector 1, and others. Finally, we use our measurements plus scaling relationships to estimate black hole masses and Eddington fractions. We show the mass estimates from different emission lines are usually in agreement within a factor of 2, but nearly a third show larger differences. We suggest using multiple mass scaling relationships to estimate black hole masses when possible, and adopting a median of the estimates as the black hole mass for individual objects. Line measurements and derived AGN properties will be used for future studies examining the relationships among quasar emission lines and their spectral energy distributions.

Subject headings: galaxies: active — galaxies: nuclei — quasars: general — ultraviolet: general

1. Introduction

Quasars are high-luminosity active galactic nuclei (AGNs), likely powered by accretion onto supermassive black holes. Through a variety of physical processes, quasars emit continuous radia-

[1]Department of Physics, Tianjin Normal University, Tianjin 300387, P. R. China; *zshang@gmail.com*

[2]Department of Astronomy, Nanjing University, Nanjing 210093, P. R. China; Key Laboratory of Astronomy and Astrophysics

[3] Department of Physics & Astronomy, Washington State University, Pullman, WA 99163

[4]Department of Physics and Astronomy, University of Wyoming, Laramie, WY 82071, USA

tion from the radio to γ-rays. The primary energy output is the "Big Blue Bump" often attributed to emission from a central accretion disk. Disk photons are reprocessed by other surrounding gas, through heating of dust in an obscuring torus as well as ionizing the broad line region (BLR) and narrow line region (NLR).

Emission lines from the BLR and NLR help cool gas ionized by the quasar, and can be diagnostic of the metallicity, ionizing continuum, the local gravitational field, and other fundamental AGN properties. While the optical-ultraviolet (UV) spectra of quasars generally resemble each other, they show variations in which systematic correlations exist among emission-line and continuum properties.

Some emission-line properties depend strongly on continuum luminosity, such as the emission-line equivalent width (EW), particularly for C IV (Baldwin 1977). This so-called Baldwin effect shows that as luminosity increases, the EW decreases. With a sample of 744 type 1 AGN spanning 6 orders of magnitude in continuum luminosity, Dietrich et al. (2002) observed an anti-correlation between the slope of the Baldwin effect and the ionization energy of the emission line ion (see also Espey & Andreadis 1999). Baskin & Laor (2004) found the correlation between EW and Eddington ratio is even stronger than the Baldwin effect, and suggested that relationship may be primary.

The strongest trends among emission lines involve a suite of correlations collectively known as "eigenvector 1." Boroson & Green (1992, hereafter BG92) employed principal component analysis (PCA) to investigate 87 low-redshift Palomar-Green quasar spectra covering λ4300-5700Å. PCA identifies orthogonal eigenvectors, which are linear combinations of input observables that correlate with each other, and which optimally account for the input data variance. The first eigenvector of BG92 (BGEV1), which accounts for the most variance in the emission-line properties, is characterized primarily by the anti-correlation between the strength of [O III] and optical Fe II, with other parameters involved, such as Hβ full width half maximum (FWHM) and asymmetry. Boroson (2002) suggested that BGEV1 is driven by Eddington ratio (L/L_{Edd}). Later, BGEV1 was expanded to include both ultraviolet emission-line properties and continuum properties in other wavebands (Sulentic et al. 2000): (1) FWHM of broad Hβ, (2) equivalent width ratio of optical Fe II to broad Hβ, (3) soft X-ray photon index, (4) C IV λ1549 broad line profile displacement at half maximum. It would be misleading to emphasize just a few line properties as defining BGEV1, when many are correlated (e.g., Si III]/C III] and others, see Wills et al. 1999), as well as features of the SED including the radio and X-ray loudness (see Kellerman et al. 1989, BG92, Corbin 1993, etc.)

Several recent papers (e.g., Hu et al. 2008; Gaskell 2009; Ferland & Baldwin 1999; Dong et al. 2009) have argued that BGEV1 can be understood in terms of the fractions of BLR clouds at high column density, which may be infalling and emit the optical Fe II lines. Cloud column density, in addition to the Eddington fraction, then governs where a quasar sits on the BGEV1 relationships. Unraveling these complicated relationships to the point that they are well understood will take more effort.

Despite indications that components of the BLR and NLR may be undergoing some degree of bulk infall or outflow, there is also strong evidence that the motions may be considered generally Keplerian (e.g., Peterson et al. 1991; Wandel et al. 1999; Onken et al. 2004) and used to estimate black hole masses. Reverberation mapping of AGNs determines the time lag between continuum changes and the response by emission lines from the BLR (e.g., Kaspi et al. 2007; Bentz et al. 2009), establishing a size scale. Doppler widths of the variable emission-line components establish velocities. Together the size and speed are used to determine the mass of the central gravitational black hole. The size of the BLR scales with continuum luminosity (e.g., Kaspi et al. 2000), allowing scaling relationships to be developed relating continuum, emission-line FWHM, and black hole mass (e.g., Vestergaard et al. 2002). Again, the emission lines and underlying continuum emission are related through fundamental quasar properties.

We have recently presented new radio-to-X-ray SEDs of a sample of 85 quasars (Shang et al. 2011). A primary virtue of these SEDs is the detailed quasi-simultaneous spectrophotometry of the optical-ultraviolet region. In this paper, we present measurements of the emission-line properties of this data set following the technique of Shang et al. (2007). Sample selection and data reduction are described in Section 2. In section 3, we use scaling relationships to estimate black hole masses as well as Eddington fractions for each quasar. We show in Section 4 that our sample displays the previously discovered relationships described above. We briefly discuss our results in Section 5, including future applications for our measurements. In this paper, we use a cosmology with H_0=70 km s^{-1} Mpc^{-1}, Ω_M=0.3, and Ω_Λ=0.7.

2. Sample, Data, and Measurements

We use the sample of Shang et al. (2011). This SED atlas has a total of 85 objects from three different subsamples which are described briefly below.

1. The 'PGX' subsample contains 22 of 23 Palomar-Green (PG) quasars in the complete sample selected by Laor et al. (1994, 1997) to study the soft-X-ray regime. This subsample is UV bright and has $z \leq 0.4$. The optical-UV region is covered by UV spectra from the Faint Object Spectrograph (FOS) on *Hubble Space Telescope* (*HST*) and quasi-simultaneous ground-based optical spectra from McDonald Observatory. See Shang et al. (2003, 2007) for details of this subsample.

2. The 'FUSE-HST' subsample has 24 objects, 17 of which come from the *FUSE* AGN program (Kriss 2000; Shang et al. 2005). This is a heterogeneous, UV-bright sample with $z < 0.5$. The SEDs for this subsample have quasi-simultaneous *FUSE* (Moos et al. 2000), *HST*, and Kitt Peak National Observatory (KPNO) observations.

3. The 'RLQ' subsample includes nearly 50 quasars originally assembled to study orientation;

all members of the sample have similar extended radio luminosity which is thought to be isotropic (Wills et al. 1995). Both lobe and core-dominant quasars are included to have a wide range in the ratio of core to extended radio emission, an indicator of the orientation. The SEDs have quasi-simultaneous *HST* and McDonald or KPNO observations. See Wills et al. (1995), Netzer et al. (1995) and Runnoe et al. (2012b) for additional details on this subsample. The blazars originally included in this sample are excluded in the SED atlas because of their variability due to optical synchrotron emission from a beamed jet.

After accounting for duplication of several quasars among the subsamples, we total 85 quasars, listed in Table 1. Figure 1 shows the redshift distribution.

Most of the quasars in our sample have quasi-simultaneous optical and UV spectra. All were observed with the *HST* Faint Object Spectrograph, primarily the radio-loud and PGX samples, or the Space Telescope Imaging Spectrograph (STIS), primarily the FUSE sample. Within a few weeks of the HST observations, low-resolution ground-based optical spectrophotometry were obtained at McDonald Observatory or KPNO. These quasars are bright in the optical and hence the host galaxy contamination is negligible as shown by Shang et al. (2011).

The combined ultraviolet-optical spectra were corrected for Galactic extinction following the empirical mean extinction law of Cardelli et al. (1989) and the values of $E(B-V)$ from Schlegel, Finkbeiner, & Davis (1998), assuming $R_V = A_V/E(B-V) = 3.1$. Then the spectra were shifted to the rest-frame using the redshift of [O III] $\lambda5007$. See Shang et al. (2011) for details.

These reddening-calibrated, redshift-calibrated spectra were divided into several main spectral regions: Ly$\alpha\,\lambda1216$, C IV $\lambda1549$, C III] $\lambda1909$, Mg II $\lambda2798$, Hβ $\lambda4686$, and Hα $\lambda6563$. We followed the recipes of fitting procedures presented by Shang et al. (2007), although we do not include the Si IV+O IV] $\lambda1400$, and He I $\lambda5876$ regions because of low S/N ratio or missing data. Briefly, we use the IRAF package SPECFIT to find the χ^2 minimization between the observed and model spectra. Each model spectrum consisted of a power-law component and several Gaussian components. A pseudo-continuum template of Fe II emission lines was added upon the power-law component in Mg II and Hβ regions. The templates of optical and ultraviolet Fe II emission lines were derived from the narrow line Seyfert 1 I Zw1 (BG92; Vestergaard & Wilkes 2001). The templates were allowed to vary in amplitude and velocity width to match the observed spectra. Each strong, broad emission line, including individual lines in doublets C IV and Mg II, was fitted with the combined profile of two Gaussian components, to which no physical meaning is imbued, but they do reproduce observed line shapes well. The parameters of broad emission lines we measured were based on these Gaussian sums.

We define the asymmetry parameter following BG92 and Shang et al. (2007):

$$\mathrm{Asymm} = \frac{\lambda_c(3/4) - \lambda_c(1/4)}{\mathrm{FWHM}}. \tag{1}$$

where $\lambda_c(3/4)$ and $\lambda_c(1/4)$ are the wavelength centers of 3/4 and 1/4 peak flux cuts, respectively. A positive value indicates excess light in the blue wing of the line.

We provide our measurements of emission lines in Table 2-6. The distributions of some emission-line parameters of this sample are shown in Figure 3-5.

3. $M_{\rm BH}$ and L_{Bol}/L_{Edd}

Two fundamental parameters can be readily estimated from our measurements: black hole mass and Eddington fraction. We use the scaling relationships for single epoch data from Vestergaard & Peterson (2006) (for C IV and Hβ) and Vestergaard & Osmer (2009) (for Mg II) to estimate black hole masses:

$$\log M_{\rm BH}({\rm H}\beta) = \log\left(\left[\frac{{\rm FWHM(H}\beta)}{1000\,{\rm km\ s^{-1}}}\right]^2 \left[\frac{\lambda L_\lambda(5100{\rm \AA})}{10^{44}\,{\rm erg\ s^{-1}}}\right]^{0.50}\right) + (6.91 \pm 0.02). \quad (2)$$

$$\log M_{\rm BH}({\rm C\ IV}) = \log\left(\left[\frac{{\rm FWHM(C\ IV)}}{1000\,{\rm km\ s^{-1}}}\right]^2 \left[\frac{\lambda L_\lambda(1350{\rm \AA})}{10^{44}\,{\rm erg\ s^{-1}}}\right]^{0.53}\right) + (6.66 \pm 0.01). \quad (3)$$

$$M_{\rm BH}({\rm Mg\ II}) = 10^{6.86\pm0.55}\left[\frac{{\rm FWHM(Mg\,II)}}{1000\,{\rm km\ s^{-1}}}\right]^2 \left[\frac{\lambda L_\lambda(3000{\rm \AA})}{10^{44}\,{\rm erg\ s^{-1}}}\right]^{0.5}. \quad (4)$$

The FWHMs of the three lines and the three continuum fluxes used above are listed in Table 7. We adopt a combination of measurements, using the median of the three estimates as the adopted black hole mass for future use. When we only have two measurements, we use a linear average. We provide the individual estimates and the combined estimate in Table 8.

We compared the black hole masses calculating using different scaling relationships in Figure 6. We found that the estimates from Hβ and Mg II agree better than those from C IV and our adopted black hole masses are mostly from the estimates using Hβ or Mg II.

Moreover, we take the ratio of any two estimates for each object and plot the distribution of all the ratios in Figure 7. We note that most estimates agree within a factor of 2, but there are 1/3 of the ratios greater than 2, indicating possible larger uncertainties of estimated black hole masses using a single scaling relationship. A few show even large differences of a factor of 5-10, mostly involving an estimate from a line with bad profile or lower signal-to-noise ratio. We also note that some of the large differences are caused by 6 objects (3C 47, 3C 110, 3C 175, B2 0742+31, 3C 254, PG 1704+608) with Hβ broader than 10,000 km s^{-1}. These result in the largest black hole masses (using Hβ) in these objects, which seem to deviate from the strong agreement between the estimates from Hβ and Mg II for lower black hole masses (Fig. 6). It is unclear what physical processes may be involved in producing the extremely broad Hβ, if they are not a natural extension of the parameter

space, but all of these largest black hole masses are excluded by the median selection when obtaining our adopted black hole masses. We suggest using multiple mass scaling relationships to estimate black hole masses and adopting a reasonable combination if possible.

We are also interested in calculating the Eddington ratio, which we define as the ratio of $L_{\rm bol}$ to $L_{\rm Edd}$, where $L_{\rm Edd} = 1.25 \times 10^{38}(M_{\rm BH}/M_{\odot})$. We use integrated bolometric luminosities from Runnoe et al. (2012a), and for the 22 objects without measured bolometric luminosities, we use the recommended correction of Runnoe et al. (2012a):

$$\log(L_{bol}) = 4.74 + 0.91\log(1450L_{1450}), \tag{5}$$

These luminosities and derived Eddington fractions are listed in Table 8. It has been suggested that the integrated bolometric luminosity should be multiplied by 0.75 to correct for a viewing angle bias and anisotropic disk emission (see e.g., Nemmen & Brotherton 2010; Runnoe et al. 2012a), but we did not apply this correction for the above quantities.

4. Emission-Line Properties

We point out consistencies between our data set and some well known correlations to highlight the fact that our sample, while heterogeneous, does appear representative. Still, it is likely more appropriate for particular applications to examine particular subsamples of Shang et al. (2011) than the entire sample.

The Boroson & Green (1992) Eigenvector 1 (BGEV1) correlations are well-studied and easily observable in many quasar samples (Wills et al. 1999; Sulentic et al. 2000; Shang et al. 2003; Zamfir et al. 2010; Kovačević et al. 2010). This is the case in our sample here, as seen in Figure 8, plotting the ratio of optical Fe II to [O III] against the FWHM of Hβ.

We also plot the Baldwin effect for C IV as well as the EW of C IV versus the Eddington fraction (Fig. 9). Both correlations are present in our sample, and as others have reported the correlation is stronger in the case of the Eddington fraction (Baskin & Laor 2004).

More could be done with our sample, particularly for subsamples, although little would likely be new or ground breaking in the realm of line-line or line-continuum correlations. The real utility will be in future studies in which emission-line properties are compared to SEDs, as well as for other projects beyond the scope of the present work. In particular, the radio-loud subsample was originally selected to study orientation effects, which appear to impact black hole mass estimates (Runnoe et al. 2012b).

5. Summary

In this paper we have reported the measurements of the emission lines of a sample of 85 quasars for redshifts $0 < z < 1.5$ with detailed radio-to-X-ray SEDs. The sample, although heterogeneous, appears to be representative of bright quasars in the low-to-moderate redshift universe for both radio-loud and radio-quiet subclasses.

We have used self-consistent scaling relationships and well-determined bolometric luminosity corrections to estimate black hole masses and Eddington fractions for future applications. We have noticed that black hole masses estimated using different scaling relationships usually agree within a factor of 2, but a significant part (1/3) also shows larger difference of a factor of 2-10. We suggest that a reasonable combination (e.g., median or average) of multiple estimates for single objects should be pursued if possible.

The line measurements as well as the derived properties of black hole mass and Eddington fraction will be useful for future studies involving the detailed SEDs of the sample objects.

This work has been supported by the National Natural Science Foundation of China (Grant No. 10773006, 11133001, and 10878010) and Chinese 973 Program 2007CB815405. We are also grateful for support by Tianjin Distinguished Professor Funds and the Ph. D. Programs Foundation of Ministry of Education of China (20100091110009). This work was also supported by NASA through grant HST-GO-10717.01-A, Spitzer-GO-20084, and Grant No. NNG05GD03G.

REFERENCES

Baldwin, J. A. 1977, ApJ, 214, 679

Baskin, A. & Laor, A. 2004, MNRAS, 350, L31

Bentz, M. C., Walsh, J. L., Barth, A. J., et al. 2009, ApJ, 705, 199

Boroson, T. A, & Green, R. F. 1992, ApJS, 80, 109 (BG92)

Cardelli, J. A., Clayton, G. C., & Mathis, J. S., 1989, ApJ, 345, 245

Corbin, M. R. 1993, ApJ, 403, L9

Dietrich, M., Hamann, F., Shields, J. C., Constantin, A., Vestergaard, M., Chaffee, F., Foltz, C. B., & Junkkarinen, V. T., 2002, ApJ, 581, 912

Dong, X.-B., Wang, T.-G., Wang, J.-G., et al. 2009, ApJ, 703, L1

Gaskell, C. M. 2009, New A Rev., 53, 140

Espey, B. R., & Andreadis, S. 1999, in ASP Conf. Series 162, Quasars and Cosmology, ed. G. J. Ferland, & J. A. Baldwin (San Francisco: ASP), 351

Ferland, G. J., & Baldwin, J. A. 1999, ASP Conf. Series 162, Quasars and Cosmology (San Francisco: ASP)

Hu, C., Wang, J.-M., Ho, L. C., et al. 2008, ApJ, 687, 78

Kaspi, S., Smith, P. S., Netzer, H., Maoz, D., Jannuzi, B. T., & Giveon, U. 2000, ApJ, 533, 631

Kaspi, S., Brandt, W. N., Maoz, D., et al. 2007, ApJ, 659, 997

Kellermann, K. I., Sramek, R., Schmidt, M., Shaffer, D. B., & Green, R. 1989, AJ, 98, 1195

Kovačević, J., Popović, L. Č., & Dimitrijević, M. S. 2010, ApJS, 189, 15

Kriss, G. J. 2000, in ASP conf. Series 224, Probing the Physics of Active Galactic Nuclei, ed. B. M. Peterson, R. W. Pogge, & R. S. Polidan (San Francisco: ASP), 45

Laor, A., Fiore, F., Elvis, M., Wilkes, B. J., & McDowell, J. C. 1994, ApJ, 435, 611 The soft x-ray properties of a complete sample of optically selected quasars. 1: First results

Laor, A., Fiore, F., Elvis, M., Wilkes, B. J., & McDowell, J. C. 1997, ApJ, 477, 93

Moos, H. W., et al. 2000, ApJ, 538, L1

Nemmen, R. S., & Brotherton, M. S. 2010, MNRAS, 408, 1598

Netzer, H., Brotherton, M. S., Wills, B. J., Han, M., Wills, D., Baldwin, J. A., Ferland, G. J., & Browne, I. W. A. 1995, ApJ, 448, 27

Onken, C. A., Ferrarese, L., Merritt, D., et al. 2004, ApJ, 615, 645

Peterson, B. M., Balonek, T. J., Barker, E. S., et al. 1991, ApJ, 368, 119

Runnoe, J. C., Brotherton, M. S., & Shang, Z. 2012, MNRAS, 422, 478

Runnoe, J. C. et al., 2012, submitted.

Schlegel, D. J., Finkbeiner, D. P., & Davis, M. 1998, ApJ, 500, 525

Shang, Z., Wills, B. J., Robinson, E. L., Wills, D., Laor, A., Xie, B., & Yuan, J. 2003, ApJ, 586, 52

Shang, Z, Brotherton, M. S., Green, R. F., Kriss, G. A., Scott, J., Quijano, J. K., Blaes, O., Hubeny, I., Hutchings, J., Kaiser, M. E., Koratkar, A., Oegerle, W., Zheng, W. 2005, ApJ, 619, 41

Shang, Z., Wills, B. J., Wills, D., & Brotherton, M. S. 2007, AJ, 134, 294

Shang, Z., Brotherton, M. S., Wills, B. J., et al. 2011, ApJS, 196, 2

Sulentic, J. W., Marziani, P., & Dultzin-Hacyan, D. 2000, ARA&A, 38, 521

Vestergaard, M. & Wilkes, B. 2001, ApJS, 134, 1

Vestergaard, M. 2002, ApJ, 571, 733

Vestergaard, M., & Peterson, B. M. 2006, ApJ, 641, 689

Vestergaard, M., & Osmer, P. S. 2009, ApJ, 699, 800

Wandel, A., Peterson, B. M., & Malkan, M. A. 1999, ApJ, 526, 579

Wills, B. J., et al. 1995, ApJ, 447, 139

Wills, B. J., Laor, A., Brotherton, M. S., et al. 1999, ApJ, 515, L53

Zamfir, S., Sulentic, J. W., Marziani, P., & Dultzin, D. 2010, MNRAS, 403, 1759

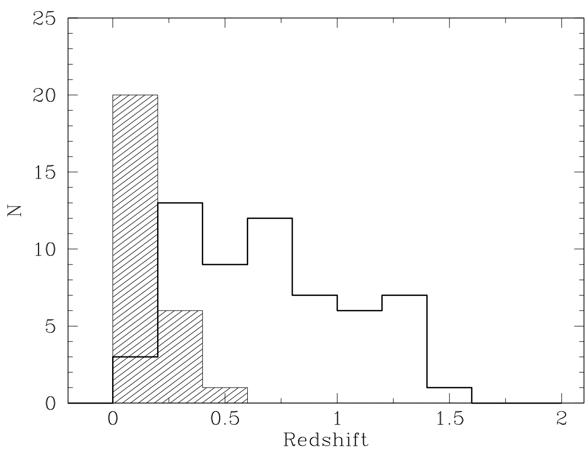

Fig. 1.— Distribution of the sample redshift. The shaded area is for radio-quiet objects, and the thick line is for radio-loud objects.

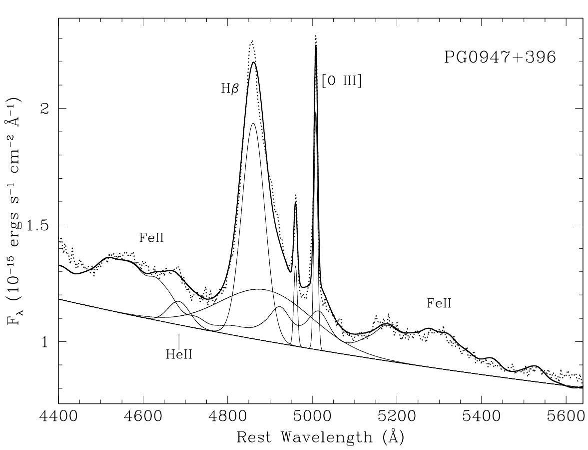

Fig. 2.— Example of model fitting to the spectra in Hβ region. Shown with the data (dotted-line) are the fitting results (thick solid line), and individual components (thin solid lines) including two Gaussians for Hβ, single Gaussian for [O III], Fe II template, and power-law continuum. He II is also modeled in this object, but it is not important in most objects.

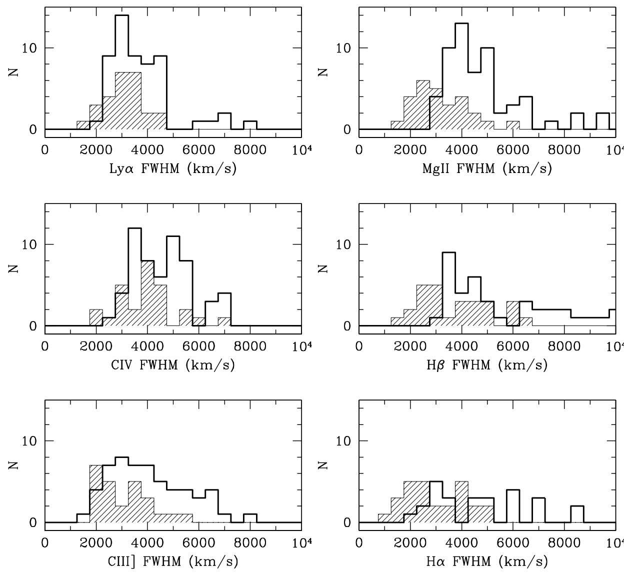

Fig. 3.— Distribution of emission-line FWHM. The shaded area is for radio-quiet objects, and the thick line is for radio-loud objects.

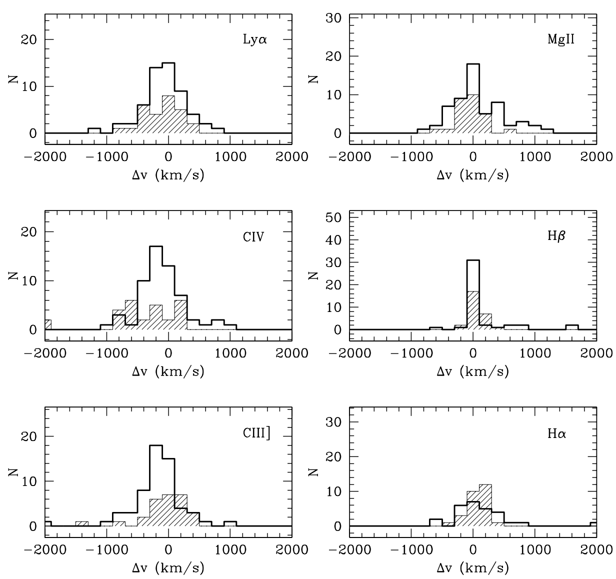

Fig. 4.— Distribution of the emission-line shift relative to [O III] λ5007. The shaded area is for radio-quiet objects, and the thick line is for radio-loud objects.

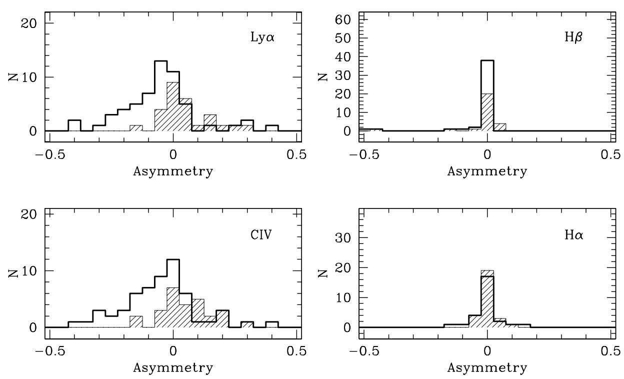

Fig. 5.— Distribution of emission-line asymmetry. The shaded area is for radio-quiet objects, and the thick line is for radio-loud objects. See §2 for definition of the asymmetry parameter.

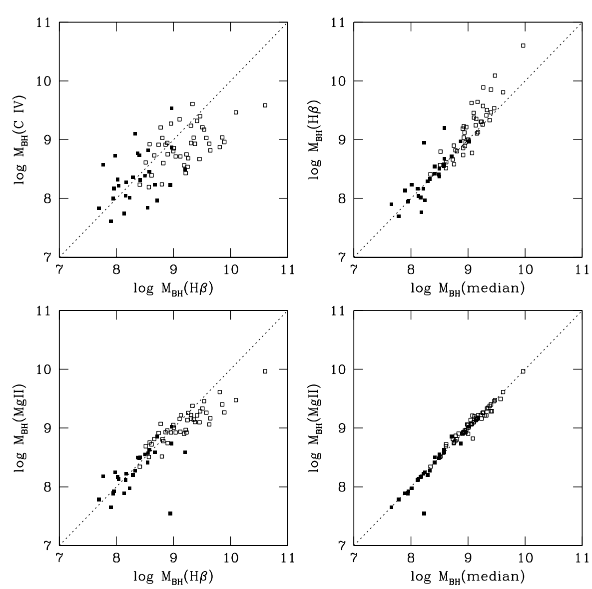

Fig. 6.— Comparison of black hole masses estimated using different scaling relationships. M$_{BH}$(median) is our adopted value.

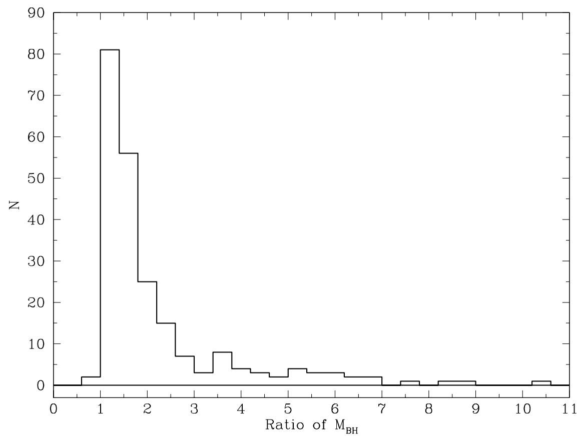

Fig. 7.— Distribution of the ratio of black hole masses estimated using different scaling relationships.

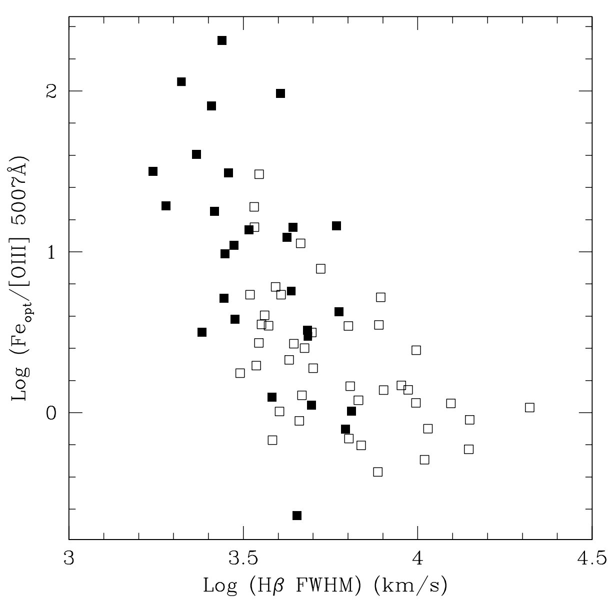

Fig. 8.— Eigenvector 1 correlation in our sample. Open squares are radio-loud objects and filled squares are radio-quiet objects.

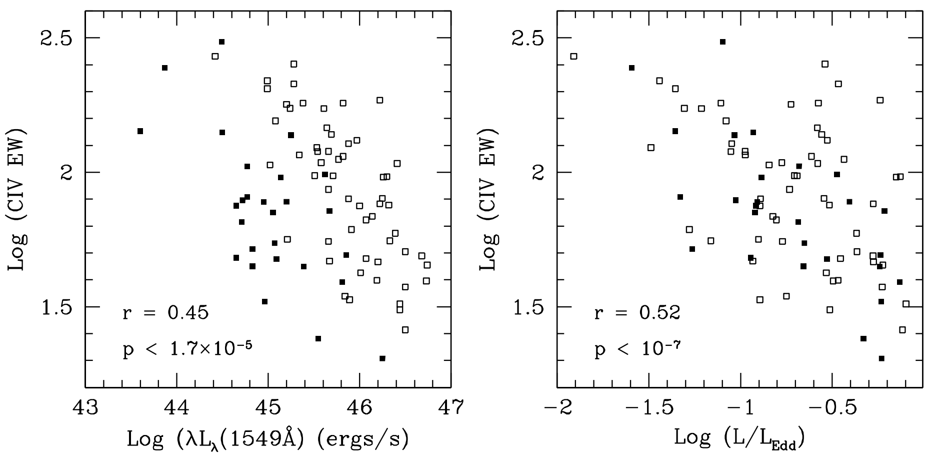

Fig. 9.— Baldwin effect and EW−L/L_{Edd} relationship in our sample. Open squares are radio-loud objects and filled squares are radio-quiet objects. The *r* and *p* are the Pearson correlation coefficient and the two-tailed probability of a correlation arising by chance, respectively.

Table 1. The Sample

ID	Name	Other Name	RA(J2000)	DEC(J2000)	z[a]	E(B−V)[b]	R[c]	SampleID
1	MC2 0042+101		00:44:58.72	+10:26:53.7	0.5870	0.068	840	RLQ
2	PG 0052+251		00:54:52.10	+25:25:38.0	0.1544	0.047	0.34	FUSE
3	PKS 0112−017	UM 310	01:15:17.10	−01:27:04.6	1.3743	0.062	2819	RLQ
4	3C 37		01:18:18.49	+02:58:06.0	0.6661	0.039	5550	RLQ
5	3C 47		01:36:24.40	+20:57:27.0	0.4250	0.061	6570	RLQ
6	4C 01.04	PHL 1093	01:39:57.25	+01:31:46.2	0.2634	0.029	2556	RLQ
7	4C 10.06	PKS 0214+10	02:17:07.66	+11:04:10.1	0.4075	0.109	472	RLQ
8	PKS 0403−13		04:05:34.00	−13:08:13.7	0.5700	0.058	5413	RLQ
9	3C 110	PKS 0414−06	04:17:16.70	−05:53:45.0	0.7749	0.043	477	RLQ
10	3C 175	PKS 0710+11	07:13:02.40	+11:46:14.7	0.7693	0.147	978	RLQ
11	3C 186		07:44:17.45	+37:53:17.1	1.0630	0.050	2131	RLQ
12	B2 0742+31		07:45:41.67	+31:42:56.6	0.4616	0.068	591	RLQ
13	IRAS F07546+3928	FBQS J075800.0+392029	07:58:00.05	+39:20:29.1	0.0953	0.066	0.25	FUSE
14	3C 207		08:40:47.59	+13:12:23.6	0.6797	0.093	4238	RLQ
15	PG 0844+349	TON 951	08:47:42.40	+34:45:04.0	0.0643	0.037	0.07	FUSE
16	PKS 0859−14		09:02:16.83	−14:15:30.9	1.3320	0.062	2683	RLQ
17	3C 215		09:06:31.90	+16:46:11.4	0.4108	0.040	2328	RLQ
18	4C 39.25	B2 0923+39	09:27:03.01	+39:02:20.9	0.6946	0.014	4512	RLQ
19	4C 40.24		09:48:55.34	+40:39:44.6	1.2520	0.014	8699	RLQ
20	PG 0947+396		09:50:48.39	+39:26:50.5	0.2057	0.019	0.31	FUSE,PGX
21	PG 0953+414		09:56:52.40	+41:15:22.0	0.2338	0.013	0.61	FUSE,PGX
22	4C 55.17		09:57:38.18	+55:22:57.8	0.8990	0.009	5525	RLQ
23	3C 232		09:58:20.95	+32:24:02.2	0.5297	0.015	736	RLQ
24	PG 1001+054		10:04:20.09	+05:13:00.5	0.1603	0.016	1.12	PGX
25	4C 22.26	PKS 1002+22	10:04:45.74	+22:25:19.4	0.9760	0.039	1817	RLQ
26	4C 41.21		10:10:27.52	+41:32:38.9	0.6124	0.015	820	RLQ
27	4C 20.24	PKS 1055+20	10:58:17.90	+19:51:50.9	1.1135	0.025	4152	RLQ
28	PG 1100+772	3C 249.1	11:04:13.69	+76:58:58.0	0.3114	0.034	444	FUSE,RLQ
29	PG 1103−006	PKS 1103−006	11:06:31.77	−00:52:52.5	0.4234	0.044	868	RLQ
30	3C 254		11:14:38.48	+40:37:20.3	0.7363	0.015	5139	RLQ
31	PG 1114+445		11:17:06.40	+44:13:33.0	0.1440	0.016	0.11	PGX
32	PG 1115+407		11:18:30.20	+40:25:53.0	0.1541	0.016	0.33	PGX
33	PG 1116+215	TON 1388	11:19:08.60	+21:19:18.0	0.1759	0.023	0.73	PGX
34	4C 12.40	MRC 1118+128	11:21:29.79	+12:36:17.4	0.6836	0.029	1071	RLQ
35	PKS 1127−14		11:30:07.05	−14:49:27.4	1.1870	0.037	7581	RLQ
36	3C 263		11:39:57.04	+65:47:49.4	0.6464	0.011	997	RLQ
37	MC2 1146+111		11:48:47.89	+10:54:59.4	0.8614	0.043	358	RLQ
38	4C 49.22	LB 02136	11:53:24.46	+49:31:08.8	0.3333	0.021	2268	RLQ
39	TEX 1156+213		11:59:26.20	+21:06:55.0	0.3480	0.027	238	RLQ
40	PG 1202+281	GQ COM	12:04:42.10	+27:54:11.0	0.1651	0.021	1.09	PGX
41	4C 64.15		12:17:41.85	+64:07:07.8	1.3000	0.019	2365	RLQ
42	PG 1216+069		12:19:20.88	+06:38:38.4	0.3319	0.022	4.64	PGX
43	PG 1226+023	3C 273	12:29:06.70	+02:03:08.6	0.1576	0.021	1667	FUSE,PGX,RLQ
44	4C 30.25	B2 1248+30	12:50:25.55	+30:16:39.3	1.0610	0.016	831	RLQ
45	3C 277.1		12:52:26.35	+56:34:19.7	0.3199	0.010	3354	RLQ
46	PG 1259+593		13:01:12.90	+59:02:06.4	0.4769	0.008	0.02	FUSE

Table 1—Continued

ID	Name	Other Name	RA(J2000)	DEC(J2000)	z[a]	E(B−V)[b]	R[c]	SampleID
47	3C 281		13:07:54.00	+06:42:14.3	0.6017	0.039	1683	RLQ
48	PG 1309+355	TON 1565	13:12:17.77	+35:15:21.2	0.1823	0.012	23.81	PGX
49	PG 1322+659		13:23:49.54	+65:41:48.0	0.1684	0.019	0.16	FUSE,PGX
50	3C 288.1		13:42:13.18	+60:21:42.9	0.9631	0.018	2660	RLQ
51	PG 1351+640	IRAS F13517+6400	13:53:15.81	+63:45:45.4	0.0882	0.020	1.24	FUSE
52	B2 1351+31		13:54:05.35	+31:39:01.9	1.3260	0.017	888	RLQ
53	PG 1352+183		13:54:35.60	+18:05:17.2	0.1510	0.019	0.24	PGX
54	4C 19.44		13:57:04.43	+19:19:07.4	0.7192	0.060	2632	RLQ
55	4C 58.29		13:58:17.63	+57:52:04.9	1.3740	0.010	453	RLQ
56	PG 1402+261	TON 182	14:05:16.19	+25:55:34.9	0.1650	0.016	0.30	PGX
57	PG 1411+442		14:13:48.30	+44:00:14.0	0.0895	0.008	0.14	PGX
58	PG 1415+451		14:17:00.80	+44:56:06.0	0.1143	0.009	0.27	PGX
59	PG 1425+267	TON 202	14:27:35.54	+26:32:13.6	0.3637	0.019	206	PGX
60	PG 1427+480		14:29:43.00	+47:47:26.0	0.2203	0.017	0.03	PGX
61	PG 1440+356	MRK 478	14:42:07.46	+35:26:22.9	0.0773	0.014	0.18	PGX
62	PG 1444+407		14:46:45.90	+40:35:05.0	0.2673	0.014	0.10	PGX
63	PG 1512+370	4C 37.43	15:14:43.04	+36:50:50.4	0.3700	0.022	717	PGX
64	PG 1534+580	MRK 290	15:35:52.36	+57:54:09.2	0.0303	0.015	1.37	FUSE
65	PG 1543+489	IRAS F15439+4855	15:45:30.20	+48:46:09.0	0.4000	0.018	1.36	PGX
66	PG 1545+210	3C 323.1	15:47:43.54	+20:52:16.7	0.2642	0.042	1000	RLQ
67	B2 1555+33		15:57:29.94	+33:04:47.0	0.9420	0.038	975	RLQ
68	B2 1611+34	DA 406	16:13:41.06	+34:12:47.9	1.3945	0.018	5825	RLQ
69	3C 334		16:20:21.92	+17:36:24.0	0.5553	0.041	1294	RLQ
70	PG 1626+554		16:27:56.00	+55:22:31.0	0.1317	0.006	0.10	PGX
71	OS 562		16:38:13.45	+57:20:24.0	0.7506	0.013	2248	RLQ
72	PKS 1656+053		16:58:33.45	+05:15:16.4	0.8890	0.159	1268	RLQ
73	PG 1704+608	3C 351	17:04:41.37	+60:44:30.5	0.3730	0.023	666	FUSE,RLQ
74	MRK 506		17:22:39.90	+30:52:53.0	0.0428	0.031	3.11	FUSE
75	4C 34.47	B2 1721+34	17:23:20.80	+34:17:57.9	0.2055	0.037	419	FUSE
76	4C 73.18		19:27:48.49	+73:58:01.6	0.3027	0.133	1587	RLQ
77	MRK 509	IRAS F20414−1054	20:44:09.74	−10:43:24.5	0.0345	0.057	0.58	FUSE
78	4C 06.69	PKS 2145+06	21:48:05.46	+06:57:38.6	1.0002	0.080	2102	RLQ
79	4C 31.63	B2 2201+31A	22:03:14.97	+31:45:38.3	0.2952	0.124	853	RLQ
80	PG 2214+139	MRK 304	22:17:12.26	+14:14:21.1	0.0657	0.073	0.04	FUSE
81	PKS 2216−03	4C −03.79	22:18:52.04	−03:35:36.9	0.8993	0.095	1708	RLQ
82	3C 446		22:25:47.26	−04:57:01.4	1.4040	0.075	21719	RLQ
83	4C 11.69	PKS 2230+11	22:32:36.41	+11:43:50.9	1.0370	0.072	5992	RLQ
84	PG 2251+113	PKS 2251+11	22:54:10.40	+11:36:38.3	0.3253	0.086	291	RLQ
85	PG 2349−014	PKS 2349−10	23:51:56.13	−01:09:13.3	0.1740	0.027	556	FUSE

[a]Redshift from Shang et al. (2011).

[b]Galactic Extinction from NED (http://nedwww.ipac.caltech.edu/) based on Schlegel, Finkbeiner, & Davis (1998).

[c]Radio loudness, $R = f(5\,GHz)/f(4215\text{Å})$, calculated using our data (Shang et al. 2011).

Table 2. Parameters of Strong Emission Lines Lyα and N V.

ID	Object	Lyα λ1216					N V λ1240[a]	
		Flux	EW	FWHM	Δv	Asymm	Flux	EW
1	MC2 0042+101	88^{+7}_{-6}	$290.1^{+85.8}_{-61.5}$	3185^{+55}_{-55}	−135	$-0.317^{+0.025}_{-0.023}$	1.	1.5
2	PG 0052+251	3078^{+124}_{-107}	$130.6^{+11.0}_{-10.2}$	3520^{+30}_{-30}	−230	$-0.065^{+0.006}_{-0.006}$	126^{+151}_{-73}	$5.5^{+7.1}_{-6.5}$
3	PKS 0112−017	43^{+4}_{-4}	$52.9^{+8.1}_{-7.4}$	2690^{+50}_{-40}	−410	$-0.023^{+0.015}_{-0.011}$	10^{+7}_{-4}	$12.5^{+10.0}_{-9.1}$
4	3C 37	158^{+6}_{-5}	$320.1^{+50.4}_{-41.1}$	2710^{+20}_{-15}	−30	$-0.197^{+0.011}_{-0.007}$	8^{+9}_{-5}	$17.6^{+22.8}_{-18.5}$
5	3C 47	395^{+39}_{-33}	$282.8^{+102.6}_{-69.3}$	4475^{+100}_{-100}	−360	$-0.199^{+0.018}_{-0.013}$	5	3.5
6	4C 01.04	129^{+14}_{-12}	$157.4^{+49.6}_{-36.0}$	4375^{+240}_{-225}	−325	$-0.195^{+0.018}_{-0.019}$	40^{+22}_{-14}	$49.6^{+40.3}_{-29.8}$
7	4C 10.06	934^{+80}_{-67}	$133.9^{+27.7}_{-22.7}$	2670^{+40}_{-45}	75	$-0.116^{+0.017}_{-0.016}$	76^{+93}_{-44}	$11.1^{+16.3}_{-13.3}$
8	PKS 0403−13	309^{+14}_{-12}	$139.5^{+15.6}_{-13.9}$	3405^{+20}_{-25}	415	$-0.071^{+0.004}_{-0.005}$	41^{+21}_{-14}	$18.7^{+11.4}_{-10.2}$
9	3C 110	554^{+29}_{-25}	$107.8^{+11.0}_{-10.0}$	4050^{+160}_{-165}	−185	$-0.207^{+0.013}_{-0.012}$	12^{+9}_{-5}	$2.4^{+1.9}_{-1.7}$
10	3C 175	384^{+44}_{-36}	$109.4^{+20.1}_{-17.9}$	6760^{+155}_{-145}	530	$0.151^{+0.037}_{-0.033}$	19^{+27}_{-12}	$5.4^{+8.5}_{-7.6}$
11	3C 186	75^{+4}_{-4}	$90.1^{+10.0}_{-9.1}$	3510^{+170}_{-165}	30	$0.052^{+0.005}_{-0.006}$	10^{+6}_{-4}	$12.3^{+8.9}_{-8.0}$
12	B2 0742+31	1016^{+29}_{-26}	$179.5^{+13.0}_{-12.0}$	4335^{+25}_{-35}	−800	$-0.168^{+0.005}_{-0.003}$	78^{+42}_{-28}	$13.9^{+8.4}_{-7.7}$
13	IRAS F07546+3928	2780^{+48}_{-42}	$193.1^{+8.8}_{-8.4}$	2805^{+5}_{-5}	−360	$-0.005^{+0.001}_{-0.000}$	304^{+84}_{-63}	$21.4^{+6.8}_{-6.4}$
14	3C 207	102^{+7}_{-6}	$100.7^{+16.2}_{-13.9}$	2800^{+30}_{-30}	140	$-0.039^{+0.005}_{-0.003}$	10^{+10}_{-5}	$10.0^{+11.6}_{-10.1}$
15	PG 0844+349	3666^{+403}_{-334}	$103.9^{+27.6}_{-21.6}$	3200^{+80}_{-75}	125	$0.040^{+0.013}_{-0.010}$	405^{+463}_{-235}	$11.7^{+16.4}_{-13.2}$
16	PKS 0859−14	139^{+18}_{-14}	$70.5^{+16.6}_{-14.0}$	4240^{+95}_{-95}	5	$-0.006^{+0.006}_{-0.003}$	36^{+29}_{-17}	$18.9^{+18.3}_{-15.5}$
17	3C 215	192^{+12}_{-10}	$203.7^{+47.3}_{-35.8}$	3700^{+75}_{-70}	−110	$-0.159^{+0.007}_{-0.009}$	3	3.2
18	4C 39.25	436^{+16}_{-14}	$91.5^{+6.0}_{-5.6}$	4350^{+30}_{-30}	815	$-0.036^{+0.005}_{-0.003}$	37^{+21}_{-14}	$8.0^{+4.9}_{-4.7}$
19	4C 40.24	74^{+4}_{-4}	$201.1^{+37.4}_{-30.1}$	2625^{+20}_{-25}	−515	$-0.112^{+0.015}_{-0.014}$	6^{+7}_{-3}	$16.6^{+22.4}_{-17.9}$
20	PG 0947+396	931^{+43}_{-37}	$114.3^{+10.7}_{-9.8}$	3125^{+25}_{-25}	−300	$-0.130^{+0.008}_{-0.004}$	96^{+68}_{-41}	$12.1^{+9.5}_{-8.7}$
21	PG 0953+414	2633^{+83}_{-72}	$84.1^{+4.6}_{-4.4}$	2700^{+15}_{-10}	−55	$-0.054^{+0.007}_{-0.004}$	251^{+137}_{-91}	$8.2^{+4.8}_{-4.6}$
22	4C 55.17	33^{+3}_{-2}	$49.0^{+6.7}_{-6.1}$	2385^{+30}_{-25}	340	$-0.097^{+0.015}_{-0.027}$	4^{+5}_{-2}	$5.8^{+7.3}_{-6.7}$
23	3C 232	281^{+19}_{-16}	$79.9^{+9.0}_{-8.3}$	3110^{+45}_{-40}	−275	$-0.086^{+0.015}_{-0.013}$	...	...
24	PG 1001+054	432^{+17}_{-15}	$107.7^{+11.2}_{-10.0}$	3350^{+55}_{-50}	−465	$0.049^{+0.003}_{-0.002}$	215^{+31}_{-25}	$54.3^{+11.4}_{-10.2}$
25	4C 22.26	106^{+6}_{-5}	$152.1^{+21.2}_{-18.4}$	4130^{+50}_{-50}	135	$-0.249^{+0.008}_{-0.007}$	9^{+8}_{-5}	$13.6^{+13.6}_{-11.7}$
26	4C 41.21	889^{+23}_{-20}	$138.8^{+7.0}_{-6.7}$	3870^{+15}_{-15}	80	$-0.037^{+0.003}_{-0.002}$	77^{+34}_{-23}	$12.3^{+5.8}_{-5.5}$
27	4C 20.24	261^{+9}_{-8}	$227.0^{+25.6}_{-22.3}$	2555^{+10}_{-15}	100	$-0.031^{+0.002}_{-0.003}$	20^{+14}_{-8}	$17.5^{+14.1}_{-12.4}$
28	PG 1100+772	1477^{+102}_{-87}	$84.7^{+10.5}_{-9.5}$	3790^{+115}_{-110}	240	$-0.089^{+0.013}_{-0.013}$	54^{+47}_{-26}	$3.1^{+3.0}_{-2.7}$
29	PG 1103−006	344^{+52}_{-42}	$85.5^{+25.8}_{-20.4}$	3250^{+120}_{-105}	235	$-0.002^{+0.026}_{-0.023}$	74^{+81}_{-40}	$18.7^{+25.3}_{-20.4}$
30	3C 254	154^{+7}_{-6}	$177.0^{+22.1}_{-19.2}$	4360^{+45}_{-45}	−100	$-0.026^{+0.006}_{-0.007}$	12^{+10}_{-6}	$14.4^{+13.8}_{-12.3}$
31	PG 1114+445	969^{+40}_{-34}	$146.7^{+14.1}_{-12.7}$	3040^{+20}_{-20}	250	$0.095^{+0.007}_{-0.006}$	132^{+62}_{-44}	$20.1^{+11.0}_{-10.0}$
32	PG 1115+407	1140^{+113}_{-94}	$76.2^{+12.3}_{-11.1}$	3685^{+65}_{-65}	−185	$0.235^{+0.029}_{-0.032}$	227^{+183}_{-111}	$15.7^{+14.2}_{-12.8}$
33	PG 1116+215	4379^{+184}_{-158}	$98.7^{+6.7}_{-6.4}$	4375^{+25}_{-30}	−385	$-0.035^{+0.002}_{-0.002}$	777^{+287}_{-208}	$18.2^{+7.3}_{-7.0}$
34	4C 12.40	103^{+9}_{-8}	$144.2^{+32.4}_{-25.9}$	3025^{+60}_{-60}	−470	$-0.245^{+0.017}_{-0.018}$	...	...
35	PKS 1127−14	88^{+15}_{-12}	$66.9^{+20.7}_{-16.7}$	4390^{+435}_{-355}	−210	$-0.009^{+0.027}_{-0.026}$	9^{+8}_{-5}	$7.1^{+7.9}_{-6.5}$
36	3C 263	728^{+24}_{-21}	$106.8^{+6.2}_{-5.9}$	2795^{+10}_{-15}	−280	$-0.042^{+0.002}_{-0.002}$	36^{+34}_{-18}	$5.5^{+5.4}_{-5.1}$
37	MC2 1146+111	59^{+6}_{-5}	$108.2^{+20.6}_{-17.8}$	3445^{+110}_{-105}	230	$0.049^{+0.028}_{-0.028}$	...	...
38	4C 49.22	421^{+25}_{-21}	$146.6^{+20.9}_{-18.0}$	4255^{+50}_{-55}	110	$-0.071^{+0.005}_{-0.005}$	51^{+39}_{-23}	$18.3^{+16.4}_{-14.2}$
39	TEX 1156+213	419^{+19}_{-17}	$121.4^{+11.4}_{-10.4}$	3355^{+40}_{-35}	−375	$0.311^{+0.007}_{-0.007}$	33^{+30}_{-16}	$9.8^{+9.6}_{-8.8}$
40	PG 1202+281	904^{+38}_{-32}	$382.7^{+78.4}_{-59.7}$	2650^{+15}_{-15}	−235	$0.055^{+0.004}_{-0.004}$	138^{+57}_{-40}	$58.9^{+36.6}_{-28.3}$
41	4C 64.15	54^{+5}_{-4}	$101.2^{+18.5}_{-15.9}$	7990^{+280}_{-280}	225	$0.016^{+0.009}_{-0.009}$	...	...
42	PG 1216+069	1005^{+34}_{-29}	$126.4^{+8.3}_{-7.8}$	2980^{+10}_{-15}	85	$-0.063^{+0.003}_{-0.005}$	...	...
43	PG 1226+023	19309^{+1142}_{-975}	$69.2^{+6.1}_{-5.8}$	3245^{+30}_{-40}	−235	$-0.116^{+0.013}_{-0.014}$	500^{+418}_{-234}	$1.8^{+1.6}_{-1.5}$
44	4C 30.25	65^{+3}_{-2}	$199.4^{+22.3}_{-19.7}$	3365^{+25}_{-20}	−210	$-0.016^{+0.001}_{-0.001}$	2^{+2}_{-1}	$4.7^{+5.9}_{-5.2}$
45	3C 277.1	...	...	...	...	...	...	...
46	PG 1259+593	663^{+58}_{-49}	$55.9^{+7.2}_{-6.7}$	11350^{+265}_{-265}	−895	$0.000^{+0.007}_{-0.006}$	23^{+22}_{-11}	$2.0^{+2.0}_{-1.9}$
47	3C 281	223^{+15}_{-12}	$123.6^{+15.8}_{-14.2}$	2885^{+30}_{-40}	−245	$-0.148^{+0.017}_{-0.015}$	9^{+8}_{-4}	$5.3^{+5.1}_{-4.6}$
48	PG 1309+355	1030^{+45}_{-38}	$81.2^{+6.2}_{-5.8}$	2070^{+10}_{-20}	480	$0.379^{+0.007}_{-0.005}$	112^{+66}_{-46}	$8.9^{+5.7}_{-5.4}$
49	PG 1322+659	931^{+64}_{-54}	$79.6^{+9.8}_{-8.9}$	3275^{+50}_{-45}	−365	$0.013^{+0.010}_{-0.010}$	82^{+93}_{-46}	$7.3^{+9.0}_{-8.1}$
50	3C 288.1	60^{+5}_{-4}	$61.3^{+7.9}_{-7.3}$	3010^{+110}_{-100}	560	$0.042^{+0.022}_{-0.021}$	...	...
51	PG 1351+640	3248^{+111}_{-97}	$189.9^{+17.6}_{-15.8}$	2190^{+10}_{-10}	200	$0.023^{+0.003}_{-0.005}$	253^{+170}_{-105}	$15.0^{+11.6}_{-10.4}$
52	B2 1351+31	32^{+4}_{-4}	$77.0^{+17.5}_{-15.1}$	3070^{+100}_{-95}	−875	$-0.389^{+0.042}_{-0.038}$	...	...
53	PG 1352+183	1363^{+100}_{-85}	$124.5^{+19.1}_{-16.6}$	3035^{+50}_{-40}	−60	$0.044^{+0.016}_{-0.013}$	159^{+155}_{-91}	$15.0^{+16.8}_{-14.6}$
54	4C 19.44	645^{+24}_{-21}	$142.9^{+11.8}_{-10.9}$	2400^{+10}_{-10}	65	$-0.020^{+0.001}_{-0.002}$	28^{+33}_{-15}	$6.2^{+8.1}_{-7.4}$
55	4C 58.29	117^{+14}_{-11}	$71.6^{+14.6}_{-12.6}$	4535^{+135}_{-125}	−60	$-0.052^{+0.016}_{-0.013}$	13^{+14}_{-8}	$8.1^{+10.4}_{-8.9}$
56	PG 1402+261	1968^{+169}_{-142}	$77.0^{+10.9}_{-9.9}$	2215^{+20}_{-30}	−100	$0.172^{+0.070}_{-0.061}$	287^{+269}_{-157}	$11.7^{+12.1}_{-11.0}$
57	PG 1411+442	4277^{+302}_{-250}	$162.7^{+24.7}_{-21.4}$	1825^{+10}_{-0}	195	$0.001^{+0.000}_{-0.000}$	534^{+522}_{-231}	$20.8^{+23.4}_{-20.4}$
58	PG 1415+451	1630^{+46}_{-40}	$148.9^{+10.9}_{-10.0}$	2975^{+10}_{-20}	−60	$0.215^{+0.008}_{-0.005}$	410^{+75}_{-59}	$38.5^{+9.0}_{-8.3}$
59	PG 1425+267	586^{+38}_{-33}	$115.8^{+16.7}_{-14.5}$	7075^{+165}_{-160}	−260	$0.058^{+0.002}_{-0.003}$	95^{+57}_{-40}	$19.5^{+13.8}_{-12.1}$
60	PG 1427+480	885^{+56}_{-47}	$106.6^{+12.8}_{-11.5}$	2730^{+20}_{-20}	320	$-0.011^{+0.001}_{-0.002}$	38^{+31}_{-18}	$4.7^{+4.3}_{-3.8}$
61	PG 1440+356	5025^{+208}_{-177}	$116.7^{+10.6}_{-9.7}$	1720^{+5}_{-5}	−90	$0.001^{+0.001}_{-0.002}$	731^{+327}_{-217}	$17.5^{+9.1}_{-8.3}$
62	PG 1444+407	679^{+47}_{-40}	$64.7^{+7.2}_{-6.7}$	3410^{+55}_{-50}	−220	$0.279^{+0.008}_{-0.010}$	248^{+78}_{-59}	$24.2^{+8.8}_{-8.2}$
63	PG 1512+370	487^{+11}_{-9}	$85.5^{+3.3}_{-3.2}$	3155^{+15}_{-10}	20	$0.282^{+0.002}_{-0.002}$	100^{+18}_{-14}	$18.5^{+3.7}_{-3.6}$
64	PG 1534+580	2192^{+107}_{-91}	$140.6^{+17.9}_{-15.6}$	2320^{+15}_{-20}	−70	$0.169^{+0.020}_{-0.020}$	166^{+156}_{-84}	$10.9^{+11.7}_{-10.2}$
65	PG 1543+489	650^{+50}_{-43}	$111.5^{+16.7}_{-14.7}$	3455^{+115}_{-105}	−550	$0.171^{+0.010}_{-0.012}$	91^{+73}_{-48}	$15.9^{+14.5}_{-12.9}$
66	PG 1545+210	1599^{+72}_{-62}	$194.8^{+22.2}_{-19.6}$	3285^{+25}_{-30}	80	$-0.058^{+0.009}_{-0.009}$	75^{+92}_{-43}	$9.3^{+12.9}_{-11.3}$

Table 2—Continued

ID	Object	Lyα λ1216 Flux	EW	FWHM	Δv	Asymm	N V λ1240[a] Flux	EW
67	B2 1555+33	40^{+3}_{-3}	$122.0^{+28.2}_{-22.1}$	3060^{+60}_{-60}	−280	$-0.163^{+0.011}_{-0.009}$	7^{+5}_{-3}	$22.8^{+19.3}_{-16.0}$
68	B2 1611+34	60^{+6}_{-5}	$65.2^{+11.9}_{-10.4}$	3295^{+75}_{-70}	400	$-0.388^{+0.021}_{-0.017}$	4^{+4}_{-2}	$4.3^{+5.2}_{-4.7}$
69	3C 334	532^{+39}_{-33}	$122.0^{+17.0}_{-15.2}$	4005^{+110}_{-100}	50	$-0.037^{+0.017}_{-0.018}$	9	2.1
70	PG 1626+554	2001^{+93}_{-79}	$93.3^{+7.7}_{-7.2}$	3940^{+30}_{-30}	−30	$0.021^{+0.005}_{-0.003}$	369^{+145}_{-104}	$17.6^{+7.8}_{-7.3}$
71	OS 562	204^{+13}_{-11}	$65.6^{+6.6}_{-6.1}$	3070^{+20}_{-30}	−85	$0.011^{+0.004}_{-0.004}$	39^{+20}_{-13}	$12.9^{+7.1}_{-6.7}$
72	PKS 1656+053	51^{+24}_{-18}	$15.5^{+8.7}_{-7.7}$	10975^{+1820}_{-1760}	−660	$0.000^{+0.077}_{-0.031}$	3	0.8
73	PG 1704+608	714^{+39}_{-34}	$63.8^{+5.8}_{-5.4}$	6590^{+120}_{-115}	−1140	$-0.246^{+0.006}_{-0.004}$	53^{+55}_{-31}	$4.9^{+5.4}_{-5.1}$
74	MRK 506	2223^{+80}_{-69}	$135.4^{+11.7}_{-10.7}$	4205^{+30}_{-35}	305	$0.037^{+0.004}_{-0.003}$	496^{+126}_{-96}	$30.8^{+9.7}_{-8.8}$
75	4C 34.47	2545^{+65}_{-56}	$258.4^{+20.4}_{-18.5}$	3115^{+10}_{-10}	−145	$0.023^{+0.001}_{-0.000}$	342^{+107}_{-79}	$35.4^{+13.6}_{-12.3}$
76	4C 73.18	...	...	...	...	...	...	...
77	MRK 509	15546^{+569}_{-495}	$157.8^{+16.3}_{-14.5}$	4470^{+45}_{-50}	−405	$0.015^{+0.002}_{-0.003}$	1000^{+728}_{-475}	$10.4^{+8.6}_{-7.7}$
78	4C 06.69	294^{+30}_{-25}	$64.0^{+10.9}_{-9.7}$	4385^{+230}_{-215}	−240	$0.021^{+0.011}_{-0.012}$	34^{+41}_{-19}	$7.5^{+10.1}_{-9.0}$
79	4C 31.63	2361^{+150}_{-128}	$71.9^{+7.0}_{-6.6}$	4095^{+75}_{-75}	−25	$-0.031^{+0.015}_{-0.014}$	66^{+68}_{-35}	$2.1^{+2.2}_{-2.1}$
80	PG 2214+139	4559^{+631}_{-516}	$91.7^{+26.7}_{-21.1}$	3545^{+125}_{-115}	240	$0.074^{+0.018}_{-0.016}$	515^{+570}_{-294}	$10.5^{+14.2}_{-11.5}$
81	PKS 2216−038	272^{+16}_{-14}	$107.0^{+13.1}_{-11.7}$	3945^{+45}_{-45}	230	$-0.174^{+0.010}_{-0.008}$	23^{+24}_{-13}	$9.3^{+10.7}_{-9.6}$
82	3C 446	38^{+2}_{-2}	$109.9^{+12.4}_{-11.0}$	2670^{+20}_{-25}	80	$-0.102^{+0.007}_{-0.005}$	4^{+3}_{-2}	$12.7^{+9.4}_{-8.3}$
83	4C 11.69	173^{+11}_{-9}	$77.9^{+8.0}_{-7.5}$	2625^{+20}_{-20}	100	$-0.049^{+0.007}_{-0.010}$	5^{+4}_{-2}	$2.2^{+2.0}_{-1.9}$
84	PG 2251+113	1228^{+43}_{-37}	$130.1^{+9.8}_{-9.1}$	3575^{+25}_{-15}	−275	$0.238^{+0.015}_{-0.016}$	168^{+65}_{-48}	$18.1^{+8.0}_{-7.4}$
85	PG 2349−014	1527^{+52}_{-45}	$143.1^{+11.2}_{-10.3}$	6175^{+85}_{-85}	−335	$0.026^{+0.003}_{-0.003}$	104^{+77}_{-46}	$9.9^{+8.1}_{-7.4}$

Note. — Flux — observed-frame flux in 10^{-15}erg s^{-1} cm^{-2} . EW — rest-frame equivalent width. FWHM — in km s^{-1}. Asymm — asymmetry parameter defined as Asymm = $[\lambda_c(\frac{3}{4}) - \lambda_c(\frac{1}{4})]$/FWHM . If the S/N ratio is too low, no reasonable flux and EW errors can be measured, therefore the flux and EW without errors are less reliable. Δv — line peak velocity shift (km s^{-1}) relative to the systematic redshift . The error for Δv depends on the uncertainty of the redshift .

[a]The values are for the sum of the doublet. Each single line is assumed to have the same shape as Lyα .

Table 3. Parameters of Strong Emission Lines C IV, C III], and Si III]

		C IV λ1549[a]					C III] λ1909				Si III] λ1892[b]	
ID	Object	Flux	EW	FWHM	Δv	Asymm	Flux	EW	FWHM	Δv	Flux	EW
1	MC2 0042+101	62^{+6}_{-5}	$218.9^{+42.5}_{-32.0}$	4195^{+245}_{-210}	−185	$-0.150^{+0.038}_{-0.034}$	5^{+2}_{-2}	$21.8^{+11.9}_{-10.1}$	2760^{+275}_{-240}	−115	2^{+2}_{-1}	$7.7^{+10.1}_{-8.6}$
2	PG 0052+251	2181^{+122}_{-101}	$137.6^{+11.3}_{-10.3}$	5815^{+175}_{-170}	−255	$-0.133^{+0.013}_{-0.010}$	261^{+22}_{-18}	$22.5^{+2.3}_{-2.2}$	3820^{+140}_{-130}	−170	42^{+19}_{-14}	$3.5^{+1.7}_{-1.7}$
3	PKS 0112−017	20^{+2}_{-2}	$30.8^{+4.1}_{-3.8}$	5030^{+550}_{-460}	−325	$0.214^{+0.014}_{-0.018}$	6^{+1}_{-1}	$11.6^{+2.7}_{-2.6}$	6085^{+380}_{-370}	−760	0.3	0.5
4	3C 37	97^{+4}_{-3}	$252.6^{+21.5}_{-18.4}$	3360^{+55}_{-50}	−170	$-0.124^{+0.008}_{-0.005}$	17^{+4}_{-3}	$52.7^{+19.8}_{-15.5}$	3765^{+235}_{-215}	45	0.1	0.3
5	3C 47	212^{+15}_{-12}	$172.9^{+17.9}_{-16.0}$	5450^{+150}_{-145}	−435	$0.108^{+0.035}_{-0.030}$	41^{+7}_{-6}	$49.5^{+11.8}_{-10.5}$	3765^{+340}_{-290}	−720	0.9	1.1
6	4C 01.04	174^{+15}_{-12}	$270.4^{+53.3}_{-39.0}$	6665^{+380}_{-350}	0	$-0.102^{+0.023}_{-0.017}$	38^{+9}_{-7}	$63.0^{+23.6}_{-19.4}$	6470^{+635}_{-610}	45	···	···
7	4C 10.06	599^{+57}_{-45}	$114.6^{+15.6}_{-13.7}$	3785^{+155}_{-155}	−270	$0.009^{+0.033}_{-0.028}$	75^{+20}_{-16}	$20.9^{+7.3}_{-6.5}$	3195^{+335}_{-285}	−430	1.6	0.4
8	PKS 0403−13	213^{+9}_{-7}	$138.3^{+8.1}_{-7.6}$	3325^{+35}_{-40}	305	$-0.081^{+0.009}_{-0.012}$	36^{+5}_{-4}	$29.7^{+5.6}_{-5.2}$	3215^{+115}_{-110}	420	···	···
9	3C 110	363^{+25}_{-21}	$107.8^{+10.1}_{-9.3}$	5700^{+350}_{-310}	−305	$-0.215^{+0.029}_{-0.028}$	56^{+12}_{-10}	$27.6^{+7.4}_{-6.7}$	6680^{+520}_{-525}	−60	0.5	0.3
10	3C 175	159^{+22}_{-17}	$55.6^{+9.1}_{-8.4}$	6915^{+1085}_{-1130}	1075	$0.205^{+0.032}_{-0.019}$	31^{+7}_{-5}	$14.1^{+3.4}_{-3.3}$	6405^{+540}_{-530}	915	···	···
11	3C 186	40^{+4}_{-3}	$66.5^{+8.6}_{-7.8}$	6290^{+465}_{-415}	−185	$-0.059^{+0.027}_{-0.024}$	11^{+3}_{-2}	$23.6^{+7.1}_{-6.5}$	8140^{+630}_{-620}	−750	0.5	1.2
12	B2 0742+31	550^{+23}_{-20}	$127.8^{+7.7}_{-7.2}$	4890^{+135}_{-120}	−855	$-0.172^{+0.013}_{-0.013}$	167^{+14}_{-12}	$46.0^{+5.0}_{-4.8}$	5580^{+150}_{-145}	−375	···	···
13	IRAS F07546+3928	1641^{+78}_{-63}	$105.3^{+6.9}_{-6.5}$	3035^{+30}_{-35}	160	$0.000^{+0.001}_{-0.001}$	411^{+39}_{-32}	$23.7^{+2.8}_{-2.7}$	2390^{+35}_{-40}	−105	36^{+34}_{-21}	$2.1^{+2.0}_{-2.0}$
14	3C 207	76^{+5}_{-4}	$86.3^{+7.8}_{-7.1}$	4935^{+135}_{-130}	225	$-0.083^{+0.012}_{-0.013}$	11^{+2}_{-2}	$14.9^{+4.3}_{-3.9}$	3240^{+325}_{-295}	−290	···	···
15	PG 0844+349	1333^{+83}_{-66}	$48.2^{+3.7}_{-3.5}$	4550^{+120}_{-110}	−105	$-0.066^{+0.010}_{-0.011}$	405^{+48}_{-41}	$17.8^{+2.6}_{-2.5}$	5300^{+195}_{-180}	310	47^{+43}_{-26}	$2.0^{+2.0}_{-1.9}$
16	PKS 0859−14	60^{+3}_{-2}	$48.9^{+2.6}_{-2.5}$	4520^{+90}_{-80}	−830	$-0.156^{+0.008}_{-0.006}$	18^{+2}_{-1}	$20.2^{+2.1}_{-2.1}$	4795^{+130}_{-120}	40	0.1	0.1
17	3C 215	153^{+7}_{-5}	$204.6^{+13.4}_{-12.4}$	5605^{+90}_{-85}	−50	$-0.099^{+0.013}_{-0.015}$	19^{+3}_{-3}	$40.2^{+9.8}_{-8.6}$	2550^{+150}_{-135}	−130	0.3	0.6
18	4C 39.25	257^{+10}_{-8}	$80.0^{+4.0}_{-3.8}$	4775^{+95}_{-85}	775	$-0.215^{+0.009}_{-0.007}$	25^{+3}_{-3}	$10.6^{+1.6}_{-1.6}$	4210^{+205}_{-200}	360	2^{+3}_{-1}	$0.8^{+1.3}_{-1.2}$
19	4C 40.24	38^{+1}_{-1}	$131.4^{+6.2}_{-5.7}$	4920^{+50}_{-45}	−240	$-0.034^{+0.003}_{-0.002}$	4^{+1}_{-1}	$18.7^{+3.7}_{-3.4}$	2885^{+120}_{-110}	40	1.1	4.8
20	PG 0947+396	590^{+55}_{-44}	$95.7^{+12.8}_{-11.3}$	3925^{+180}_{-170}	−150	$-0.169^{+0.020}_{-0.005}$	90^{+20}_{-15}	$18.8^{+4.9}_{-4.6}$	3580^{+270}_{-235}	−315	17^{+17}_{-10}	$3.6^{+3.7}_{-3.5}$
21	PG 0953+414	1150^{+86}_{-68}	$49.4^{+4.5}_{-4.3}$	3810^{+90}_{-100}	−95	$-0.013^{+0.002}_{-0.003}$	157^{+23}_{-19}	$9.9^{+1.6}_{-1.6}$	2215^{+65}_{-70}	40	43^{+20}_{-15}	$2.6^{+1.3}_{-1.3}$
22	4C 55.17	20^{+2}_{-1}	$34.6^{+3.8}_{-3.6}$	6420^{+675}_{-1130}	630	$-0.419^{+0.021}_{-0.063}$	···	···	···	···	···	···
23	3C 232	100^{+6}_{-5}	$33.5^{+2.3}_{-2.2}$	7145^{+350}_{-340}	155	$0.000^{+0.013}_{-0.014}$	54^{+13}_{-10}	$19.4^{+5.2}_{-4.9}$	4320^{+465}_{-380}	−300	11^{+11}_{-7}	$4.0^{+4.1}_{-3.9}$
24	PG 1001+054	272^{+22}_{-18}	$75.1^{+8.1}_{-7.4}$	3130^{+90}_{-90}	−695	$0.305^{+0.080}_{-0.108}$	79^{+9}_{-8}	$26.9^{+3.9}_{-3.7}$	2725^{+60}_{-60}	−205	32^{+9}_{-7}	$10.7^{+3.4}_{-3.2}$
25	4C 22.26	78^{+4}_{-3}	$180.9^{+13.6}_{-12.4}$	5015^{+150}_{-140}	100	$-0.276^{+0.012}_{-0.008}$	9^{+1}_{-1}	$29.3^{+4.4}_{-4.1}$	3705^{+115}_{-110}	−115	0.7	2.4
26	4C 41.21	451^{+18}_{-15}	$96.0^{+5.1}_{-4.9}$	3800^{+60}_{-60}	−195	$-0.056^{+0.007}_{-0.005}$	70^{+8}_{-6}	$21.6^{+2.9}_{-2.8}$	2390^{+65}_{-50}	75	17^{+7}_{-5}	$5.3^{+2.2}_{-2.1}$
27	4C 20.24	137^{+5}_{-5}	$185.3^{+13.1}_{-11.7}$	3525^{+55}_{-50}	−20	$-0.059^{+0.004}_{-0.002}$	16^{+2}_{-2}	$26.8^{+4.4}_{-4.1}$	3115^{+100}_{-90}	145	3^{+2}_{-1}	$4.9^{+3.1}_{-2.9}$
28	PG 1100+772	951^{+45}_{-38}	$79.7^{+4.8}_{-4.6}$	4775^{+245}_{-210}	145	$0.021^{+0.014}_{-0.015}$	151^{+38}_{-30}	$17.2^{+5.1}_{-4.8}$	4670^{+440}_{-385}	90	4.7	0.5
29	PG 1103−006	181^{+30}_{-22}	$55.3^{+11.6}_{-10.3}$	4515^{+355}_{-325}	145	$0.009^{+0.056}_{-0.027}$	85^{+16}_{-13}	$34.7^{+8.3}_{-7.6}$	7125^{+440}_{-425}	25	0.1	0.1
30	3C 254	107^{+5}_{-4}	$172.4^{+12.8}_{-11.6}$	5205^{+185}_{-175}	−215	$-0.179^{+0.018}_{-0.017}$	12^{+2}_{-2}	$26.3^{+6.0}_{-5.5}$	1820^{+195}_{-135}	−115	···	···
31	PG 1114+445	498^{+36}_{-29}	$81.1^{+7.7}_{-7.1}$	3935^{+135}_{-130}	−40	$0.053^{+0.019}_{-0.019}$	152^{+22}_{-18}	$25.3^{+4.5}_{-4.2}$	4045^{+205}_{-190}	155	25^{+20}_{-13}	$4.1^{+3.4}_{-3.2}$
32	PG 1115+407	519^{+89}_{-66}	$47.6^{+10.1}_{-9.0}$	4585^{+415}_{-365}	−600	$0.095^{+0.055}_{-0.052}$	115^{+20}_{-16}	$13.7^{+2.9}_{-2.7}$	2380^{+245}_{-205}	55	28^{+18}_{-12}	$3.3^{+2.2}_{-2.1}$
33	PG 1116+215	2161^{+137}_{-113}	$71.8^{+5.9}_{-5.6}$	3865^{+115}_{-110}	−605	$0.060^{+0.015}_{-0.013}$	534^{+59}_{-49}	$24.6^{+3.4}_{-3.2}$	3625^{+155}_{-150}	−80	135^{+54}_{-40}	$6.1^{+2.7}_{-2.5}$
34	4C 12.40	59^{+5}_{-4}	$97.2^{+11.4}_{-10.4}$	5300^{+210}_{-210}	−10	$-0.059^{+0.020}_{-0.014}$	11^{+3}_{-2}	$27.5^{+10.0}_{-8.5}$	4620^{+475}_{-465}	−430	0.9	2.3
35	PKS 1127−14	30^{+5}_{-4}	$25.9^{+4.9}_{-4.6}$	3695^{+300}_{-265}	370	$-0.114^{+0.039}_{-0.000}$	$12^{+1}_{-1.}$	$12.4^{+0.8}_{-0.7}$	5075^{+70}_{-65}	−430	$3^{+1}_{-1.}$	$2.9^{+0.6}_{-0.6}$
36	3C 263	345^{+20}_{-16}	$75.5^{+5.4}_{-5.1}$	3310^{+60}_{-60}	−285	$-0.032^{+0.006}_{-0.012}$	48^{+9}_{-7}	$13.8^{+3.0}_{-2.8}$	2615^{+150}_{-130}	−270	7^{+8}_{-4}	$2.0^{+2.2}_{-2.1}$
37	MC2 1146+111	21^{+3}_{-2}	$46.8^{+7.6}_{-6.9}$	3715^{+245}_{-215}	−565	$-0.037^{+0.042}_{-0.029}$	9^{+1}_{-1}	$20.3^{+3.9}_{-3.7}$	3540^{+180}_{-160}	−25	···	···
38	4C 49.22	379^{+18}_{-15}	$178.8^{+15.1}_{-13.3}$	4535^{+100}_{-95}	65	$-0.144^{+0.011}_{-0.010}$	47^{+6}_{-5}	$26.7^{+4.4}_{-4.1}$	3920^{+130}_{-125}	320	20^{+5}_{-4}	$11.5^{+3.6}_{-3.3}$
39	TEX 1156+213	302^{+25}_{-20}	$116.1^{+13.5}_{-12.1}$	3880^{+160}_{-145}	−380	$0.307^{+0.025}_{-0.026}$	46^{+6}_{-5}	$22.6^{+3.9}_{-3.7}$	5040^{+185}_{-190}	−925	···	···
40	PG 1202+281	711^{+31}_{-26}	$306.3^{+27.4}_{-23.5}$	2945^{+35}_{-25}	−835	$0.041^{+0.008}_{-0.005}$	125^{+11}_{-9}	$63.5^{+9.3}_{-8.4}$	2855^{+45}_{-50}	−780	21^{+9}_{-6}	$10.3^{+5.2}_{-4.7}$
41	4C 64.15	26^{+3}_{-2}	$68.5^{+8.0}_{-7.6}$	7245^{+400}_{-365}	−350	$-0.056^{+0.023}_{-0.012}$	3^{+1}_{-1}	$11.7^{+3.4}_{-3.2}$	4185^{+550}_{-555}	−235	0.1	0.2
42	PG 1216+069	557^{+25}_{-21}	$98.0^{+5.6}_{-5.4}$	3105^{+45}_{-40}	250	$0.223^{+0.040}_{-0.051}$	70^{+12}_{-10}	$14.9^{+2.9}_{-2.8}$	2625^{+230}_{-195}	20	···	···
43	PG 1226+023	7417^{+580}_{-467}	$32.4^{+2.9}_{-2.8}$	4530^{+165}_{-160}	−470	$-0.017^{+0.015}_{-0.009}$	1957^{+157}_{-134}	$11.2^{+1.0}_{-1.0}$	5085^{+120}_{-120}	−345	182^{+129}_{-86}	$1.0^{+0.7}_{-0.7}$
44	4C 30.25	33^{+2}_{-2}	$146.3^{+17.7}_{-14.8}$	3730^{+105}_{-105}	−280	$-0.016^{+0.015}_{-0.012}$	4^{+1}_{-1}	$23.9^{+6.1}_{-5.4}$	2660^{+140}_{-125}	−95	0.8	4.4
45	3C 277.1	164^{+8}_{-7}	$106.5^{+7.6}_{-7.0}$	3215^{+50}_{-55}	−175	$-0.080^{+0.015}_{-0.018}$	21^{+4}_{-3}	$19.2^{+4.3}_{-4.0}$	1810^{+40}_{-50}	25	5^{+3}_{-2}	$4.5^{+3.4}_{-3.2}$

Table 3—Continued

ID	Object	C IV λ1549[a]					C III] λ1909				Si III] λ1892[b]	
		Flux	EW	FWHM	Δv	Asymm	Flux	EW	FWHM	Δv	Flux	EW
46	PG 1259+593	184^{+32}_{-25}	$20.3^{+3.9}_{-3.7}$	6880^{+1085}_{-1015}	−3220	$0.086^{+0.028}_{-0.017}$	···	···	···	···	···	···
47	3C 281	149^{+16}_{-13}	$119.7^{+18.6}_{-16.1}$	4865^{+405}_{-335}	−460	$0.037^{+0.037}_{-0.034}$	14^{+4}_{-3}	$14.6^{+4.9}_{-4.5}$	1515^{+100}_{-95}	−235	5^{+4}_{-2}	$5.4^{+4.2}_{-3.8}$
48	PG 1309+355	550^{+55}_{-44}	$56.3^{+6.8}_{-6.3}$	2815^{+145}_{-130}	270	$0.410^{+0.036}_{-0.034}$	134^{+23}_{-19}	$15.9^{+3.2}_{-3.1}$	2160^{+180}_{-140}	80	23^{+20}_{-13}	$2.7^{+2.4}_{-2.3}$
49	PG 1322+659	455^{+55}_{-43}	$54.4^{+8.4}_{-7.6}$	3690^{+210}_{-195}	−425	$0.182^{+0.048}_{-0.059}$	110^{+20}_{-16}	$17.2^{+3.8}_{-3.6}$	3285^{+245}_{-220}	−195	8^{+15}_{-7}	$1.3^{+2.3}_{-2.2}$
50	3C 288.1	30^{+4}_{-3}	$42.3^{+6.3}_{-5.9}$	4015^{+250}_{-230}	−270	$0.164^{+0.044}_{-0.046}$	5^{+1}_{-1}	$10.1^{+3.0}_{-2.9}$	2585^{+240}_{-205}	95	2^{+1}_{-1}	$4.0^{+2.9}_{-2.8}$
51	PG 1351+640	1296^{+88}_{-68}	$78.6^{+7.3}_{-6.7}$	4050^{+85}_{-85}	−525	$-0.018^{+0.001}_{-0.002}$	291^{+42}_{-34}	$17.9^{+3.2}_{-3.0}$	2055^{+60}_{-60}	420	125^{+41}_{-31}	$7.7^{+2.8}_{-2.6}$
52	B2 1351+31	15^{+2}_{-1}	$47.7^{+5.9}_{-5.6}$	3690^{+510}_{-350}	−25	$-0.167^{+0.050}_{-0.047}$	3^{+1}_{-1}	$13.2^{+3.4}_{-3.1}$	4465^{+425}_{-425}	−520	0.8	3.2
53	PG 1352+183	650^{+64}_{-51}	$77.8^{+10.4}_{-9.3}$	3755^{+205}_{-190}	−450	$0.103^{+0.022}_{-0.018}$	119^{+22}_{-18}	$18.0^{+4.0}_{-3.7}$	3115^{+175}_{-155}	0	35^{+20}_{-14}	$5.2^{+3.2}_{-3.0}$
54	4C 19.44	310^{+15}_{-12}	$96.4^{+6.3}_{-5.9}$	2730^{+45}_{-50}	−145	$-0.228^{+0.010}_{-0.006}$	40^{+6}_{-5}	$17.0^{+3.1}_{-2.9}$	3575^{+205}_{-195}	−155	3^{+5}_{-2}	$1.1^{+2.0}_{-1.8}$
55	4C 58.29	49^{+2}_{-2}	$39.4^{+2.3}_{-2.3}$	5745^{+235}_{-220}	100	$-0.022^{+0.011}_{-0.010}$	11^{+2}_{-2}	$11.6^{+2.3}_{-2.2}$	5965^{+295}_{-295}	−530	1^{+1}_{-1}	$1.5^{+1.7}_{-1.6}$
56	PG 1402+261	832^{+95}_{-73}	$44.6^{+6.1}_{-5.7}$	4550^{+235}_{-225}	−765	$0.147^{+0.051}_{-0.046}$	176^{+34}_{-27}	$12.1^{+2.8}_{-2.6}$	1810^{+70}_{-60}	120	95^{+33}_{-24}	$6.4^{+2.5}_{-2.4}$
57	PG 1411+442	912^{+63}_{-49}	$44.7^{+4.0}_{-3.8}$	2040^{+35}_{-40}	155	$-0.034^{+0.004}_{-0.006}$	424^{+56}_{-45}	$25.5^{+4.1}_{-3.9}$	1765^{+20}_{-30}	−10	116^{+51}_{-34}	$6.9^{+3.3}_{-3.1}$
58	PG 1415+451	589^{+60}_{-47}	$65.5^{+9.5}_{-8.3}$	3725^{+175}_{-175}	−635	$0.091^{+0.029}_{-0.025}$	147^{+24}_{-19}	$20.5^{+4.0}_{-3.8}$	2540^{+65}_{-70}	280	100^{+23}_{-18}	$13.6^{+3.7}_{-3.5}$
59	PG 1425+267	449^{+34}_{-28}	$123.5^{+13.3}_{-12.0}$	7060^{+415}_{-375}	−845	$0.015^{+0.021}_{-0.019}$	74^{+15}_{-12}	$25.6^{+6.3}_{-5.8}$	3935^{+305}_{-270}	−230	24^{+14}_{-10}	$8.1^{+5.1}_{-4.8}$
60	PG 1427+480	463^{+28}_{-23}	$77.6^{+6.6}_{-6.0}$	2835^{+60}_{-55}	130	$-0.035^{+0.004}_{-0.007}$	72^{+16}_{-12}	$17.0^{+4.5}_{-4.2}$	2065^{+80}_{-70}	215	16^{+14}_{-8}	$3.7^{+3.4}_{-3.2}$
61	PG 1440+356	1247^{+67}_{-54}	$33.0^{+2.2}_{-2.1}$	2130^{+45}_{-35}	−545	$0.095^{+0.025}_{-0.018}$	558^{+39}_{-33}	$19.3^{+1.7}_{-1.6}$	2175^{+40}_{-40}	−85	234^{+36}_{-29}	$7.9^{+1.4}_{-1.3}$
62	PG 1444+407	199^{+24}_{-17}	$24.1^{+3.2}_{-3.1}$	4425^{+185}_{-180}	−870	$-0.014^{+0.006}_{-0.003}$	82^{+11}_{-10}	$12.0^{+1.9}_{-1.8}$	3730^{+300}_{-305}	110	54^{+11}_{-9}	$7.8^{+1.8}_{-1.7}$
63	PG 1512+370	420^{+21}_{-17}	$119.3^{+8.0}_{-7.5}$	3970^{+115}_{-100}	45	$0.212^{+0.020}_{-0.019}$	55^{+13}_{-10}	$21.9^{+5.8}_{-5.5}$	4215^{+195}_{-185}	230	9^{+9}_{-5}	$3.5^{+3.7}_{-3.5}$
64	PG 1534+580	1740^{+106}_{-85}	$142.5^{+14.0}_{-12.3}$	3790^{+70}_{-75}	−295	$0.053^{+0.013}_{-0.009}$	260^{+39}_{-31}	$29.8^{+5.5}_{-5.1}$	2215^{+50}_{-40}	135	41^{+35}_{-22}	$4.6^{+4.2}_{-4.0}$
65	PG 1543+489	209^{+10}_{-8}	$39.1^{+2.1}_{-2.1}$	5625^{+110}_{-105}	−2065	$0.144^{+0.026}_{-0.021}$	···	···	···	···	···	···
66	PG 1545+210	1047^{+53}_{-45}	$181.1^{+14.9}_{-13.4}$	4560^{+135}_{-125}	150	$0.002^{+0.014}_{-0.014}$	115^{+21}_{-17}	$25.8^{+6.3}_{-5.7}$	3040^{+200}_{-175}	−210	···	···
67	B2 1555+33	30^{+3}_{-2}	$108.5^{+14.7}_{-12.7}$	4240^{+200}_{-180}	−260	$-0.346^{+0.031}_{-0.019}$	6^{+1}_{-1}	$26.6^{+7.4}_{-6.8}$	2355^{+300}_{-215}	−505	0.2	1.0
68	B2 1611+34	36^{+4}_{-3}	$50.7^{+7.6}_{-7.0}$	4625^{+350}_{-305}	765	$-0.270^{+0.030}_{-0.015}$	5^{+2}_{-1}	$9.1^{+3.6}_{-3.3}$	3610^{+605}_{-550}	525	0.7	1.4
69	3C 334	251^{+17}_{-14}	$75.0^{+6.6}_{-6.1}$	5745^{+345}_{-310}	−20	$-0.003^{+0.014}_{-0.014}$	47^{+12}_{-9}	$18.1^{+5.4}_{-5.0}$	5530^{+520}_{-475}	−295	6^{+9}_{-4}	$2.1^{+3.6}_{-3.3}$
70	PG 1626+554	1013^{+126}_{-97}	$70.9^{+11.5}_{-10.3}$	3815^{+205}_{-195}	−295	$0.014^{+0.039}_{-0.024}$	249^{+50}_{-39}	$23.0^{+5.4}_{-5.1}$	4490^{+175}_{-175}	−175	37^{+38}_{-20}	$3.3^{+3.6}_{-3.4}$
71	OS 562	105^{+13}_{-10}	$46.4^{+7.1}_{-6.6}$	3470^{+160}_{-150}	15	$-0.140^{+0.068}_{-0.086}$	20^{+6}_{-5}	$13.1^{+4.5}_{-4.2}$	4280^{+420}_{-365}	−165	2.1	1.4
72	PKS 1656+053	···	···	···	···	···	···	···	···	···	···	···
73	PG 1704+608	496^{+42}_{-34}	$61.2^{+6.2}_{-5.8}$	4015^{+230}_{-205}	−495	$-0.043^{+0.040}_{-0.036}$	115^{+29}_{-23}	$17.1^{+4.9}_{-4.6}$	3595^{+715}_{-495}	−395	···	···
74	MRK 506	2671^{+81}_{-69}	$244.4^{+14.5}_{-13.0}$	5290^{+80}_{-75}	240	$0.020^{+0.004}_{-0.004}$	456^{+27}_{-24}	$50.8^{+4.5}_{-4.3}$	5015^{+85}_{-85}	−245	61^{+23}_{-17}	$6.7^{+2.8}_{-2.6}$
75	4C 34.47	1802^{+54}_{-46}	$213.0^{+11.2}_{-10.3}$	2855^{+30}_{-25}	−365	$0.057^{+0.009}_{-0.010}$	180^{+23}_{-18}	$28.5^{+5.1}_{-4.7}$	2385^{+60}_{-60}	−370	49^{+21}_{-15}	$7.7^{+3.7}_{-3.4}$
76	4C 73.18	1120^{+56}_{-47}	$111.8^{+8.3}_{-7.6}$	3560^{+80}_{-80}	−50	$0.000^{+0.011}_{-0.010}$	200^{+33}_{-27}	$27.8^{+5.9}_{-5.4}$	2970^{+170}_{-155}	−55	19^{+29}_{-14}	$2.7^{+4.3}_{-4.0}$
77	MRK 509	10404^{+181}_{-156}	$140.8^{+3.5}_{-3.4}$	4710^{+25}_{-25}	−725	$-0.009^{+0.002}_{-0.002}$	2001^{+80}_{-69}	$32.4^{+1.7}_{-1.6}$	3470^{+40}_{-40}	−360	276^{+69}_{-54}	$4.4^{+1.2}_{-1.1}$
78	4C 06.69	151^{+16}_{-13}	$45.2^{+5.7}_{-5.3}$	5620^{+410}_{-365}	−1005	$0.027^{+0.021}_{-0.016}$	31^{+3}_{-2}	$12.2^{+1.1}_{-1.1}$	5680^{+145}_{-150}	−115	2^{+2}_{-1}	$1.0^{+0.8}_{-0.8}$
79	4C 31.63	1109^{+123}_{-97}	$39.6^{+5.1}_{-4.8}$	4840^{+335}_{-295}	−255	$0.035^{+0.026}_{-0.022}$	306^{+70}_{-56}	$15.2^{+4.1}_{-3.8}$	6465^{+465}_{-450}	−45	18.7	0.9
80	PG 2214+139	2101^{+151}_{-124}	$51.9^{+4.6}_{-4.3}$	2690^{+105}_{-90}	125	$0.196^{+0.013}_{-0.013}$	379^{+38}_{-32}	$11.6^{+1.3}_{-1.3}$	4025^{+110}_{-110}	345	82^{+32}_{-25}	$2.5^{+1.0}_{-1.0}$
81	PKS 2216−038	121^{+14}_{-11}	$59.3^{+8.7}_{-8.0}$	3600^{+245}_{-215}	−105	$-0.290^{+0.057}_{-0.049}$	32^{+6}_{-5}	$19.2^{+4.5}_{-4.2}$	5730^{+405}_{-410}	215	4^{+6}_{-3}	$2.4^{+3.7}_{-3.5}$
82	3C 446	28^{+5}_{-4}	$76.4^{+19.1}_{-15.3}$	3390^{+300}_{-255}	145	$-0.297^{+0.076}_{-0.007}$	3^{+3}_{-2}	$9.8^{+11.1}_{-9.1}$	2250^{+835}_{-515}	−145	0.9	2.9
83	4C 11.69	66^{+6}_{-5}	$37.4^{+4.0}_{-3.8}$	3185^{+105}_{-100}	10	$-0.014^{+0.012}_{-0.005}$	15^{+4}_{-3}	$11.3^{+3.2}_{-3.0}$	3730^{+325}_{-295}	−225	···	···
84	PG 2251+113	713^{+35}_{-29}	$96.9^{+6.3}_{-5.9}$	4805^{+100}_{-100}	−435	$0.058^{+0.015}_{-0.014}$	154^{+14}_{-12}	$27.8^{+3.2}_{-3.1}$	3290^{+125}_{-110}	−285	18^{+11}_{-8}	$3.2^{+2.2}_{-2.1}$
85	PG 2349−014	1232^{+85}_{-70}	$155.4^{+17.4}_{-15.1}$	5675^{+305}_{-275}	−195	$0.041^{+0.013}_{-0.011}$	200^{+21}_{-18}	$34.1^{+5.0}_{-4.6}$	5865^{+170}_{-175}	−250	52^{+18}_{-14}	$8.7^{+3.4}_{-3.2}$

Note. — Same as Table 2 for C IV, C III], and Si III] emission lines.

[a]Flux and EW are the sum of the C IV doublet. FWHM of C IV is for a single component of the doublet

[b]Si III] is assumed to have the same FWHM and Δv as C III] .

Table 4. Parameters of Strong Emission Lines Mg II, Hβ, and [O III]

ID	Object	Mg II[a] Flux	Mg II EW	Mg II FWHM	Mg II Δv	Hβ Flux	Hβ EW	Hβ FWHM	Hβ Δv	Hβ Asymm	[O III] λ5007[b] Flux	[O III] EW	[O III] FWHM	[O III] Δv
1	MC2 0042+101	14^{+3}_{-2}	$79.1^{+20.9}_{-18.6}$	6275^{+420}_{-400}	0	8^{+3}_{-2}	$105.5^{+62.1}_{-48.1}$	8270^{+1040}_{-980}	−75	$0.000^{+0.020}_{-0.031}$	$3.9^{+0.3}_{-0.3}$	$50.4^{+12.6}_{-9.7}$	606^{+10}_{-10}	−75
2	PG 0052+251	601^{+69}_{-58}	$89.7^{+13.6}_{-12.8}$	4510^{+165}_{-165}	−160	276^{+10}_{-9}	$128.3^{+5.9}_{-5.8}$	6460^{+60}_{-70}	−15	$0.000^{+0.002}_{-0.002}$	$110.4^{+0.9}_{-0.8}$	$53.8^{+1.0}_{-1.0}$	847^{+0}_{-0}	−15
3	PKS 0112−017	7^{+2}_{-1}	$30.1^{+10.1}_{-9.3}$	4130^{+255}_{-250}	−100	…	…	…	…	…	…	…	…	…
4	3C 37	25^{+5}_{-4}	$129.6^{+41.2}_{-33.5}$	4200^{+180}_{-175}	720	15^{+2}_{-2}	$272.9^{+33.4}_{-33.4}$	4280^{+190}_{-170}	20	$0.000^{+0.013}_{-0.014}$	$5.3^{+0.2}_{-0.2}$	$105.9^{+4.0}_{-4.0}$	904^{+10}_{-10}	20
5	3C 47	56^{+9}_{-7}	$124.1^{+26.6}_{-24.4}$	7745^{+625}_{-595}	80	26^{+4}_{-3}	$153.2^{+35.6}_{-31.6}$	14005^{+755}_{-755}	10	$0.000^{+0.016}_{-0.014}$	$19.1^{+0.3}_{-0.3}$	$116.2^{+9.7}_{-8.6}$	1128^{+10}_{-0}	10
6	4C 01.04	76^{+12}_{-10}	$142.8^{+32.7}_{-29.2}$	9550^{+440}_{-425}	1170	24^{+7}_{-5}	$67.0^{+23.5}_{-21.0}$	9905^{+815}_{-790}	3220	$-0.005^{+0.019}_{-0.010}$	$13.9^{+0.6}_{-0.5}$	$39.0^{+2.9}_{-2.7}$	777^{+10}_{-10}	−75
7	4C 10.06	152^{+46}_{-35}	$67.9^{+26.9}_{-23.5}$	4670^{+450}_{-400}	165	107^{+5}_{-5}	$142.0^{+9.1}_{-8.9}$	4735^{+70}_{-70}	50	$-0.497^{+0.010}_{-0.012}$	$17.9^{+0.2}_{-0.2}$	$24.8^{+0.7}_{-0.7}$	546^{+0}_{-0}	−10
8	PKS 0403−13	35^{+11}_{-8}	$45.3^{+18.2}_{-16.4}$	3535^{+230}_{-220}	455	23^{+3}_{-2}	$68.1^{+10.6}_{-9.9}$	3735^{+85}_{-90}	820	$-0.001^{+0.006}_{-0.006}$	$6.5^{+0.3}_{-0.3}$	$19.9^{+1.5}_{-1.4}$	704^{+10}_{-10}	0
9	3C 110	58^{+13}_{-10}	$47.4^{+13.0}_{-12.0}$	5645^{+370}_{-355}	35	44^{+16}_{-13}	$106.4^{+50.8}_{-44.0}$	12450^{+1615}_{-1450}	1625	$-0.049^{+0.029}_{-0.070}$	$9.9^{+1.4}_{-1.2}$	$25.0^{+6.7}_{-5.4}$	793^{+30}_{-30}	15
10	3C 175	42^{+13}_{-10}	$28.4^{+9.4}_{-9.0}$	9515^{+1095}_{-1060}	710	67^{+6}_{-5}	$125.6^{+14.4}_{-13.9}$	20925^{+595}_{-585}	3335	$0.000^{+0.012}_{-0.010}$	$10.5^{+0.2}_{-0.2}$	$20.1^{+0.7}_{-0.7}$	567^{+0}_{-0}	10
11	3C 186	12^{+3}_{-2}	$46.7^{+14.2}_{-13.1}$	5790^{+635}_{-600}	15	…	…	…	…	…	…	…	…	…
12	B2 0742+31	189^{+20}_{-17}	$69.6^{+9.4}_{-9.0}$	6060^{+180}_{-185}	−800	133^{+7}_{-6}	$122.5^{+7.8}_{-7.7}$	10690^{+180}_{-170}	280	$-0.054^{+0.005}_{-0.003}$	$42.8^{+0.4}_{-0.3}$	$41.3^{+0.8}_{-0.8}$	532^{+0}_{-0}	−20
13	IRAS F07546	415^{+281}_{-154}	$31.3^{+25.2}_{-21.9}$	2045^{+170}_{-155}	−170	596^{+45}_{-38}	$99.5^{+9.6}_{-9.2}$	2785^{+30}_{-30}	−15	$0.000^{+0.002}_{-0.001}$	$220.0^{+3.1}_{-2.8}$	$38.0^{+1.2}_{-1.2}$	579^{+10}_{-0}	−15
14	3C 207	16^{+4}_{-3}	$33.5^{+9.3}_{-8.6}$	4140^{+280}_{-265}	225	14^{+3}_{-2}	$75.2^{+14.7}_{-14.7}$	3505^{+55}_{-60}	585	$0.000^{+0.001}_{-0.001}$	$4.2^{+0.1}_{-0.1}$	$23.3^{+0.5}_{-0.5}$	548^{+10}_{-0}	−10
15	PG 0844+349	364^{+254}_{-137}	$26.2^{+21.0}_{-18.7}$	3160^{+355}_{-335}	160	333^{+18}_{-15}	$69.3^{+4.5}_{-4.4}$	2870^{+10}_{-20}	80	$0.001^{+0.001}_{-0.001}$	$32.9^{+1.6}_{-1.3}$	$7.1^{+0.4}_{-0.4}$	615^{+10}_{-10}	80
16	PKS 0859−14	13^{+3}_{-2}	$26.0^{+6.6}_{-6.4}$	3775^{+185}_{-180}	920	$26^{+1.}_{-1.}$	$108.2^{+0.6}_{-0.6}$	4615^{+0}_{-10}	−75	$0.000^{+0.001}_{-0.001}$	$2.0^{+0.0}_{-0.0}$	$8.7^{+0.0}_{-0.0}$	778^{+0}_{-0}	−75
17	3C 215	21^{+7}_{-5}	$56.7^{+23.6}_{-21.1}$	6260^{+750}_{-670}	930	13^{+3}_{-2}	$62.0^{+16.1}_{-14.6}$	6760^{+500}_{-505}	15	$0.000^{+0.014}_{-0.012}$	$9.5^{+0.3}_{-0.3}$	$47.0^{+3.9}_{-3.6}$	716^{+10}_{-0}	15
18	4C 39.25	46^{+8}_{-6}	$34.3^{+6.6}_{-6.3}$	5075^{+235}_{-235}	750	29^{+3}_{-2}	$56.4^{+6.5}_{-6.2}$	6400^{+225}_{-210}	1520	$0.000^{+0.005}_{-0.004}$	$7.7^{+0.2}_{-0.2}$	$15.2^{+0.7}_{-0.7}$	664^{+0}_{-0}	10
19	4C 40.24	6^{+1}_{-1}	$46.7^{+10.9}_{-10.9}$	3650^{+170}_{-170}	−165	…	…	…	…	…	…	…	…	…
20	PG 0947+396	169^{+41}_{-32}	$62.9^{+20.0}_{-17.9}$	4170^{+280}_{-270}	80	96^{+11}_{-9}	$109.8^{+17.4}_{-16.3}$	4340^{+125}_{-115}	5	$0.001^{+0.006}_{-0.007}$	$19.9^{+1.4}_{-1.2}$	$23.7^{+2.9}_{-2.7}$	743^{+10}_{-20}	5
21	PG 0953+414	212^{+88}_{-51}	$23.7^{+11.2}_{-10.4}$	2700^{+165}_{-165}	235	205^{+10}_{-9}	$77.9^{+4.9}_{-4.7}$	2990^{+20}_{-20}	120	$0.001^{+0.001}_{-0.001}$	$29.6^{+1.5}_{-1.3}$	$12.0^{+0.8}_{-0.8}$	906^{+10}_{-10}	120
22	4C 55.17	4^{+2}_{-1}	$14.6^{+6.8}_{-6.3}$	3475^{+300}_{-290}	310	…	…	…	…	…	…	…	…	…
23	3C 232	122^{+9}_{-8}	$66.7^{+6.3}_{-6.1}$	4620^{+85}_{-90}	390	10^{+4}_{-3}	$15.3^{+6.0}_{-5.8}$	4655^{+795}_{-625}	25	$-0.001^{+0.036}_{-0.033}$	$35.4^{+0.7}_{-0.6}$	$55.4^{+2.0}_{-2.0}$	1121^{+0}_{-10}	25
24	PG 1001+054	62^{+30}_{-19}	$34.4^{+19.9}_{-17.6}$	2280^{+150}_{-140}	−155	56^{+1}_{-1}	$83.9^{+3.3}_{-3.2}$	2615^{+10}_{-15}	−55	$0.056^{+0.002}_{-0.001}$	$7.6^{+0.3}_{-0.3}$	$12.1^{+0.7}_{-0.7}$	1158^{+20}_{-10}	−25
25	4C 22.26	12^{+2}_{-1}	$67.5^{+15.1}_{-13.4}$	4910^{+240}_{-230}	525	…	…	…	…	…	…	…	…	…
26	4C 41.21	72^{+21}_{-15}	$54.0^{+19.2}_{-17.3}$	3060^{+180}_{-170}	−95	37^{+3}_{-3}	$101.2^{+12.5}_{-11.9}$	3445^{+70}_{-65}	0	$0.000^{+0.009}_{-0.010}$	$11.5^{+0.4}_{-0.4}$	$33.0^{+2.2}_{-2.1}$	811^{+0}_{-10}	0
27	4C 20.24	26^{+3}_{-3}	$75.5^{+12.7}_{-12.0}$	4070^{+120}_{-120}	330	…	…	…	…	…	…	…	…	…
28	PG 1100+772	205^{+52}_{-40}	$47.7^{+14.7}_{-13.5}$	6090^{+480}_{-445}	370	144^{+28}_{-23}	$99.7^{+25.5}_{-23.1}$	9390^{+555}_{-560}	−30	$0.000^{+0.012}_{-0.011}$	$57.2^{+2.3}_{-2.0}$	$42.1^{+4.1}_{-3.7}$	653^{+0}_{-10}	−30
29	PG 1103−006	69^{+19}_{-14}	$45.6^{+15.4}_{-14.1}$	4780^{+355}_{-335}	−40	28^{+3}_{-3}	$60.3^{+8.1}_{-7.8}$	5270^{+180}_{-180}	50	$0.000^{+0.006}_{-0.006}$	$5.8^{+0.5}_{-0.4}$	$13.1^{+1.5}_{-1.4}$	1382^{+30}_{-30}	50
30	3C 254	22^{+5}_{-4}	$73.6^{+23.9}_{-20.9}$	6595^{+545}_{-505}	−65	20^{+9}_{-7}	$185.2^{+112.7}_{-93.9}$	14095^{+2720}_{-2605}	−75	$0.000^{+0.069}_{-0.142}$	$12.5^{+0.9}_{-0.7}$	$116.5^{+36.5}_{-25.0}$	988^{+20}_{-15}	−75
31	PG 1114+445	188^{+60}_{-43}	$40.4^{+15.2}_{-14.0}$	4255^{+295}_{-275}	−125	192^{+7}_{-6}	$91.6^{+3.9}_{-3.8}$	4825^{+30}_{-30}	40	$-0.135^{+0.007}_{-0.007}$	$31.3^{+0.5}_{-0.4}$	$15.8^{+0.3}_{-0.3}$	706^{+0}_{-0}	−95
32	PG 1115+407	110^{+54}_{-37}	$28.2^{+19.1}_{-15.3}$	2750^{+410}_{-370}	290	81^{+7}_{-6}	$71.6^{+8.0}_{-7.6}$	1895^{+20}_{-30}	285	$-0.021^{+0.003}_{-0.002}$	$8.8^{+0.9}_{-0.8}$	$8.1^{+1.0}_{-1.0}$	822^{+20}_{-30}	30
33	PG 1116+215	447^{+59}_{-48}	$45.1^{+7.4}_{-7.0}$	2885^{+90}_{-90}	−235	318^{+9}_{-7}	$117.8^{+4.5}_{-4.4}$	2975^{+15}_{-15}	200	$-0.021^{+0.002}_{-0.000}$	$42.2^{+1.9}_{-1.7}$	$16.7^{+0.9}_{-0.9}$	1523^{+20}_{-20}	−80
34	4C 12.40	12^{+6}_{-4}	$54.6^{+36.5}_{-30.2}$	4205^{+575}_{-505}	−430	4^{+1}_{-1}	$51.9^{+14.9}_{-14.9}$	3565^{+190}_{-180}	−5	$0.000^{+0.006}_{-0.004}$	$3.2^{+0.1}_{-0.1}$	$40.9^{+1.7}_{-1.7}$	673^{+0}_{-10}	−5
35	PKS 1127−14	15^{+3}_{-2}	$30.5^{+6.8}_{-6.5}$	3725^{+145}_{-145}	325	…	…	…	…	…	…	…	…	…
36	3C 263	69^{+16}_{-13}	$34.8^{+9.5}_{-9.0}$	4265^{+245}_{-230}	15	63^{+7}_{-6}	$82.1^{+10.4}_{-10.1}$	4970^{+130}_{-130}	15	$0.001^{+0.011}_{-0.011}$	$14.3^{+0.6}_{-0.5}$	$20.1^{+1.1}_{-1.0}$	727^{+10}_{-0}	15
37	MC2 1146+111	9^{+3}_{-2}	$35.0^{+12.1}_{-11.2}$	5020^{+510}_{-435}	−365	5^{+3}_{-2}	$51.2^{+40.8}_{-33.5}$	7835^{+1745}_{-1625}	15	$0.000^{+0.050}_{-0.024}$	$2.2^{+0.3}_{-0.3}$	$22.1^{+6.0}_{-4.9}$	637^{+30}_{-20}	15
38	4C 49.22	94^{+14}_{-11}	$101.6^{+22.0}_{-19.8}$	4415^{+155}_{-150}	−100	30^{+3}_{-2}	$103.2^{+13.5}_{-12.6}$	3910^{+70}_{-60}	10	$0.000^{+0.003}_{-0.003}$	$7.5^{+0.2}_{-0.2}$	$26.6^{+1.8}_{-1.7}$	579^{+10}_{-0}	10
39	TEX 1156+213	52^{+12}_{-9}	$45.1^{+12.2}_{-11.4}$	5175^{+360}_{-335}	−680	28^{+5}_{-4}	$71.6^{+14.5}_{-13.7}$	7740^{+425}_{-430}	0	$0.000^{+0.010}_{-0.010}$	$6.4^{+0.5}_{-0.4}$	$17.5^{+1.9}_{-1.8}$	734^{+10}_{-20}	0
40	PG 1202+281	212^{+11}_{-9}	$114.4^{+7.9}_{-7.7}$	3990^{+35}_{-45}	−535	109^{+8}_{-7}	$144.1^{+12.4}_{-12.0}$	4950^{+85}_{-80}	−255	$-0.427^{+0.009}_{-0.006}$	$40.5^{+0.5}_{-0.4}$	$55.9^{+1.4}_{-1.4}$	672^{+0}_{-0}	75
41	4C 64.15	4^{+1}_{-1}	$22.0^{+10.6}_{-9.3}$	5125^{+710}_{-620}	−505	…	…	…	…	…	…	…	…	…
42	PG 1216+069	80^{+31}_{-22}	$32.6^{+14.2}_{-13.2}$	3085^{+200}_{-195}	15	108^{+8}_{-7}	$80.1^{+7.2}_{-7.0}$	5950^{+125}_{-125}	265	$0.040^{+0.003}_{-0.003}$	$13.4^{+0.6}_{-0.5}$	$10.5^{+0.6}_{-0.6}$	641^{+0}_{-10}	35
43	PG 1226+023	2108^{+979}_{-654}	$23.9^{+12.4}_{-11.6}$	2935^{+240}_{-215}	−195	1432^{+104}_{-87}	$56.4^{+4.8}_{-4.7}$	3405^{+50}_{-40}	135	$-0.001^{+0.002}_{-0.002}$	$198.7^{+21.6}_{-18.2}$	$8.3^{+1.0}_{-1.0}$	1751^{+50}_{-60}	135
44	4C 30.25	8^{+2}_{-1}	$92.7^{+35.1}_{-27.6}$	4440^{+255}_{-240}	−155	…	…	…	…	…	…	…	…	…
45	3C 277.1	29^{+11}_{-7}	$48.7^{+23.1}_{-20.2}$	3380^{+245}_{-225}	−35	24^{+3}_{-3}	$109.1^{+22.1}_{-20.2}$	3835^{+155}_{-140}	0	$-0.001^{+0.013}_{-0.012}$	$33.5^{+0.4}_{-0.3}$	$159.4^{+9.8}_{-8.9}$	620^{+0}_{-10}	0
46	PG 1259+593	79^{+32}_{-22}	$22.3^{+10.7}_{-9.7}$	3650^{+375}_{-365}	−465	91^{+19}_{-15}	$108.2^{+30.8}_{-27.4}$	4035^{+195}_{-185}	45	$0.000^{+0.023}_{-0.024}$	$3.5^{+2.2}_{-1.6}$	$4.5^{+3.3}_{-2.9}$	1124^{+240}_{-230}	45
47	3C 281	33^{+7}_{-5}	$62.5^{+16.1}_{-14.9}$	5505^{+400}_{-370}	−495	16^{+4}_{-3}	$89.0^{+30.4}_{-27.2}$	7985^{+960}_{-920}	−75	$0.000^{+0.029}_{-0.030}$	$8.2^{+0.5}_{-0.4}$	$46.8^{+5.6}_{-5.0}$	877^{+10}_{-10}	−75
48	PG 1309+355	176^{+38}_{-29}	$34.1^{+8.7}_{-8.2}$	3355^{+150}_{-145}	−85	153^{+7}_{-6}	$69.0^{+3.7}_{-3.6}$	3640^{+30}_{-30}	380	$-0.457^{+0.017}_{-0.015}$	$36.4^{+0.6}_{-0.6}$	$17.1^{+0.4}_{-0.4}$	950^{+10}_{-0}	35
49	PG 1322+659	58^{+29}_{-21}	$17.6^{+11.3}_{-9.4}$	2765^{+460}_{-430}	565	76^{+5}_{-4}	$65.1^{+5.4}_{-5.2}$	3285^{+30}_{-30}	45	$-0.001^{+0.001}_{-0.001}$	$8.2^{+0.4}_{-0.3}$	$7.5^{+0.5}_{-0.5}$	509^{+10}_{-0}	45
50	3C 288.1	7^{+2}_{-2}	$22.6^{+8.3}_{-7.7}$	4320^{+390}_{-350}	165	10^{+4}_{-3}	$103.4^{+63.1}_{-50.8}$	8970^{+1310}_{-1260}	10	$0.000^{+0.031}_{-0.020}$	$7.7^{+1.0}_{-0.8}$	$85.4^{+22.8}_{-18.2}$	1785^{+60}_{-60}	10
51	PG 1351+640	418^{+418}_{-250}	$40.1^{+51.0}_{-40.1}$	1400^{+305}_{-220}	95	345^{+45}_{-37}	$44.6^{+6.6}_{-6.4}$	6205^{+285}_{-275}	10	$0.000^{+0.007}_{-0.007}$	$285.5^{+6.4}_{-5.6}$	$38.1^{+1.4}_{-1.4}$	1049^{+10}_{-0}	10
52	B2 1351+31	4^{+1}_{-1}	$33.6^{+7.4}_{-7.4}$	4205^{+235}_{-225}	−455	…	…	…	…	…	…	…	…	…
53	PG 1352+183	141^{+38}_{-28}	$42.3^{+14.5}_{-13.0}$	4175^{+290}_{-280}	−290	85^{+10}_{-8}	$84.6^{+12.2}_{-11.7}$	4210^{+70}_{-75}	50	$-0.025^{+0.002}_{-0.003}$	$9.2^{+0.9}_{-0.7}$	$9.7^{+1.1}_{-1.1}$	794^{+20}_{-20}	−65
54	4C 19.44	66^{+13}_{-10}	$48.8^{+11.8}_{-11.0}$	3105^{+130}_{-115}	−25	44^{+6}_{-5}	$89.8^{+16.3}_{-15.0}$	4575^{+170}_{-160}	−5	$0.000^{+0.010}_{-0.009}$	$38.2^{+0.6}_{-0.5}$	$78.6^{+4.7}_{-4.3}$	688^{+10}_{-0}	−5
55	4C 58.29	13^{+4}_{-3}	$28.4^{+9.1}_{-8.7}$	4830^{+460}_{-420}	−150	…	…	…	…	…	…	…	…	…
56	PG 1402+261	215^{+75}_{-45}	$31.5^{+13.3}_{-12.0}$	2460^{+125}_{-130}	295	134^{+6}_{-5}	$77.0^{+4.5}_{-4.4}$	2100^{+10}_{-10}	80	$0.002^{+0.000}_{-0.002}$	$4.0^{+0.9}_{-0.7}$	$2.5^{+0.6}_{-0.6}$	1221^{+80}_{-80}	120
57	PG 1411+442	329^{+106}_{-75}	$26.9^{+10.0}_{-9.3}$	1975^{+90}_{-90}	40	495^{+9}_{-8}	$107.6^{+2.5}_{-2.5}$	2800^{+5}_{-5}	−100	$-0.011^{+0.001}_{-0.001}$	$58.2^{+0.9}_{-0.8}$	$13.4^{+0.3}_{-0.3}$	816^{+0}_{-0}	75
58	PG 1415+451	178^{+44}_{-32}	$47.1^{+14.6}_{-13.3}$	2425^{+95}_{-90}	−35	98^{+6}_{-5}	$62.7^{+4.7}_{-4.5}$	2560^{+20}_{-20}	15	$0.027^{+0.001}_{-0.002}$	$4.1^{+0.8}_{-0.6}$	$2.7^{+0.5}_{-0.5}$	906^{+50}_{-50}	−235
59	PG 1425+267	129^{+53}_{-40}	$66.7^{+36.5}_{-30.6}$	8280^{+1090}_{-1015}	−135	71^{+8}_{-7}	$108.3^{+13.7}_{-13.3}$	9875^{+420}_{-420}	−25	$-0.134^{+0.017}_{-0.015}$	$19.7^{+0.4}_{-0.4}$	$31.6^{+1.2}_{-1.1}$	685^{+0}_{-0}	0
60	PG 1427+480	85^{+13}_{-10}	$38.2^{+6.6}_{-6.3}$	2415^{+50}_{-55}	20	74^{+3}_{-3}	$108.9^{+6.5}_{-6.3}$	2405^{+10}_{-10}	350	$-0.007^{+0.002}_{-0.000}$	$17.9^{+0.2}_{-0.2}$	$27.9^{+0.7}_{-0.7}$	671^{+0}_{-10}	0
61	PG 1440+356	470^{+177}_{-114}	$30.1^{+13.6}_{-12.3}$	1800^{+80}_{-80}	−55	273^{+6}_{-5}	$51.4^{+1.6}_{-1.5}$	1745^{+5}_{-5}	−25	$0.020^{+0.000}_{-0.003}$	$38.5^{+1.5}_{-1.3}$	$7.6^{+0.4}_{-0.3}$	952^{+10}_{-10}	−25
62	PG 1444+407	93^{+16}_{-12}	$22.7^{+4.5}_{-4.3}$	2760^{+90}_{-95}	−130	78^{+3}_{-2}	$68.1^{+2.9}_{-2.9}$	2750^{+10}_{-10}	130	$0.005^{+0.000}_{-0.001}$	$1.6^{+0.3}_{-0.2}$	$1.5^{+0.3}_{-0.3}$	870^{+40}_{-50}	70
63	PG 1512+370	106^{+19}_{-15}	$60.0^{+12.4}_{-11.8}$	6545^{+310}_{-295}	−265	72^{+7}_{-6}	$149.2^{+18.1}_{-17.4}$	7690^{+295}_{-275}	−135	$-0.115^{+0.013}_{-0.014}$	$26.4^{+0.5}_{-0.4}$	$58.4^{+2.3}_{-2.2}$	633^{+0}_{-0}	45
64	PG 1534+580	309^{+131}_{-92}	$57.2^{+33.2}_{-27.2}$	3305^{+350}_{-310}	−150	162^{+34}_{-27}	$72.7^{+19.6}_{-18.0}$	4505^{+235}_{-225}	10	$0.001^{+0.011}_{-0.007}$	$247.5^{+4.4}_{-3.9}$	$114.5^{+7.1}_{-6.5}$	854^{+0}_{-0}	10
65	PG 1543+489	65^{+10}_{-8}	$31.4^{+5.9}_{-5.7}$	1980^{+55}_{-45}	155	40^{+3}_{-3}	$60.4^{+5.7}_{-5.6}$	2320^{+25}_{-30}	155	$0.025^{+0.003}_{-0.001}$	$3.3^{+0.7}_{-0.5}$	$5.4^{+1.2}_{-1.1}$	1056^{+60}_{-60}	−670
66	PG 1545+210	174^{+34}_{-27}	$66.5^{+17.0}_{-15.4}$	5230^{+300}_{-285}	−130	99^{+4}_{-4}	$108.9^{+6.0}_{-5.8}$	6885^{+90}_{-85}	570	$0.000^{+0.002}_{-0.002}$	$36.2^{+0.5}_{-0.5}$	$41.5^{+1.1}_{-1.0}$	912^{+0}_{-10}	15

Table 4—Continued

ID	Object	Mg II[a] Flux	Mg II[a] EW	Mg II[a] FWHM	Mg II[a] Δv	Hβ Flux	Hβ EW	Hβ FWHM	Hβ Δv	Hβ Asymm	[O III] λ5007[b] Flux	[O III] λ5007[b] EW	[O III] λ5007[b] FWHM	[O III] λ5007[b] Δv
67	B2 1555+33	6^{+2}_{-2}	$57.4^{+29.9}_{-24.9}$	4650^{+500}_{-450}	665	...	...	...	...	...	...	...	...	...
68	B2 1611+34	8^{+3}_{-2}	$32.1^{+12.6}_{-11.7}$	4010^{+335}_{-305}	105	$3^{+0.}_{-0.}$	$23.3^{+0.3}_{-0.3}$	4795^{+10}_{-10}	−40	$0.000^{+0.001}_{-0.001}$	$2.4^{+0.0}_{-0.0}$	$17.4^{+0.0}_{-0.0}$	1123^{+0}_{-0}	−40
69	3C 334	70^{+26}_{-19}	$49.7^{+23.9}_{-20.7}$	4840^{+560}_{-505}	−435	33^{+7}_{-5}	$76.1^{+17.3}_{-16.5}$	6345^{+550}_{-480}	10	$0.000^{+0.025}_{-0.023}$	$16.4^{+0.5}_{-0.5}$	$40.5^{+2.3}_{-2.2}$	757^{+10}_{-0}	10
70	PG 1626+554	258^{+136}_{-90}	$45.2^{+31.4}_{-25.8}$	4155^{+580}_{-520}	35	170^{+33}_{-26}	$98.6^{+27.2}_{-23.9}$	4390^{+185}_{-180}	155	$-0.058^{+0.011}_{-0.017}$	$8.8^{+3.2}_{-2.4}$	$5.4^{+2.4}_{-2.1}$	793^{+90}_{-90}	−25
71	OS 562	18^{+4}_{-3}	$22.3^{+6.0}_{-5.7}$	3465^{+195}_{-195}	−25	19^{+13}_{-8}	$64.1^{+67.8}_{-48.0}$	3305^{+525}_{-455}	10	$0.001^{+0.014}_{-0.194}$	$4.2^{+2.1}_{-1.6}$	$14.4^{+12.9}_{-8.5}$	836^{+140}_{-130}	10
72	PKS 1656+053	21^{+3}_{-2}	$20.3^{+3.2}_{-3.1}$	3980^{+130}_{-135}	−405	13^{+4}_{-3}	$26.5^{+8.1}_{-7.8}$	3510^{+180}_{-160}	−75	$0.001^{+0.008}_{-0.006}$	$1.9^{+0.5}_{-0.4}$	$3.8^{+1.0}_{-1.0}$	983^{+70}_{-70}	−75
73	PG 1704+608	89^{+38}_{-29}	$24.4^{+11.7}_{-10.9}$	8405^{+1180}_{-1105}	230	61^{+8}_{-7}	$36.8^{+5.4}_{-5.3}$	10465^{+410}_{-410}	90	$0.000^{+0.009}_{-0.008}$	$44.3^{+0.6}_{-0.5}$	$27.7^{+0.7}_{-0.7}$	562^{+0}_{-0}	90
74	MRK 506	624^{+4}_{-3}	$155.3^{+1.4}_{-1.4}$	5130^{+45}_{-55}	−35	288^{+23}_{-19}	$103.3^{+10.7}_{-10.3}$	4840^{+105}_{-110}	−10	$0.000^{+0.006}_{-0.006}$	$95.0^{+2.6}_{-2.2}$	$35.7^{+1.8}_{-1.7}$	801^{+0}_{-10}	−10
75	4C 34.47	413^{+99}_{-77}	$87.8^{+24.8}_{-23.2}$	3175^{+100}_{-100}	−220	168^{+16}_{-13}	$124.2^{+15.7}_{-14.8}$	5015^{+135}_{-130}	−15	$0.000^{+0.007}_{-0.006}$	$119.7^{+1.5}_{-1.4}$	$92.7^{+4.2}_{-3.9}$	716^{+0}_{-0}	−15
76	4C 73.18	250^{+55}_{-41}	$43.0^{+11.3}_{-10.5}$	3345^{+130}_{-130}	380	159^{+5}_{-5}	$82.6^{+3.3}_{-3.2}$	3095^{+20}_{-20}	5	$0.000^{+0.002}_{-0.002}$	$45.0^{+0.5}_{-0.5}$	$24.4^{+0.4}_{-0.4}$	652^{+0}_{-0}	5
77	MRK 509	2479^{+180}_{-146}	$66.1^{+6.2}_{-5.9}$	3680^{+50}_{-40}	−225	1636^{+74}_{-63}	$142.7^{+9.2}_{-8.9}$	3825^{+40}_{-30}	0	$0.000^{+0.002}_{-0.002}$	$915.1^{+8.4}_{-7.6}$	$83.6^{+2.3}_{-2.2}$	756^{+0}_{-0}	0
78	4C 06.69	24^{+4}_{-3}	$19.6^{+4.0}_{-3.8}$	4220^{+165}_{-155}	−60	20^{+4}_{-3}	$36.4^{+9.6}_{-8.9}$	4015^{+230}_{-220}	−75	$-0.001^{+0.009}_{-0.008}$	$22.2^{+0.8}_{-0.7}$	$42.9^{+3.4}_{-3.2}$	1018^{+10}_{-10}	−75
79	4C 31.63	309^{+161}_{-102}	$30.7^{+19.3}_{-16.9}$	4055^{+515}_{-470}	0	179^{+9}_{-8}	$72.6^{+4.4}_{-4.3}$	3395^{+30}_{-20}	710	$0.000^{+0.001}_{-0.001}$	$14.8^{+1.3}_{-1.1}$	$6.4^{+0.6}_{-0.6}$	1153^{+25}_{-30}	40
80	PG 2214+139	798^{+733}_{-431}	$39.0^{+45.8}_{-36.1}$	6220^{+2195}_{-1645}	−5	732^{+58}_{-48}	$112.1^{+11.7}_{-11.2}$	5845^{+125}_{-115}	5	$0.000^{+0.003}_{-0.003}$	$77.6^{+5.3}_{-4.5}$	$12.4^{+1.1}_{-1.1}$	793^{+10}_{-20}	5
81	PKS 2216−038	42^{+10}_{-8}	$37.5^{+10.9}_{-10.1}$	3555^{+180}_{-170}	100	46^{+8}_{-7}	$82.7^{+18.5}_{-17.2}$	4415^{+220}_{-210}	5	$0.000^{+0.013}_{-0.011}$	$16.9^{+0.8}_{-0.7}$	$31.7^{+2.8}_{-2.6}$	646^{+10}_{-10}	5
82	3C 446	5^{+3}_{-2}	$21.9^{+13.7}_{-12.6}$	3955^{+580}_{-510}	330	...	...	...	...	...	...	...	...	...
83	4C 11.69	20^{+7}_{-5}	$24.5^{+9.5}_{-8.8}$	3675^{+280}_{-260}	−60	...	...	...	...	...	...	...	...	...
84	PG 2251+113	154^{+66}_{-47}	$36.1^{+18.9}_{-16.8}$	4110^{+500}_{-450}	0	151^{+14}_{-12}	$96.5^{+12.0}_{-11.4}$	4060^{+105}_{-110}	−535	$0.001^{+0.007}_{-0.006}$	$41.8^{+1.8}_{-1.5}$	$28.1^{+2.0}_{-1.9}$	900^{+0}_{-10}	−75
85	PG 2349−014	415^{+107}_{-84}	$108.8^{+41.4}_{-34.6}$	4825^{+605}_{-510}	−335	129^{+16}_{-13}	$101.2^{+16.1}_{-15.2}$	6325^{+250}_{-240}	−5	$0.000^{+0.008}_{-0.007}$	$39.2^{+1.2}_{-1.1}$	$32.3^{+1.8}_{-1.7}$	709^{+10}_{-0}	−5

Note. — Same as Table 2 for Mg II, Hβ, and [O III] emission lines.

[a]Flux and EW are the sum of the Mg II doublet. FWHM of Mg II is for a single component of the doublet

[b]Non-zero Δv reflects the uncertainty of the redshift (Shang et al. 2011).

Table 5. Parameters of UV and Optical Fe Blends, and the Small Blue Bump

		Optical Fe II[a]		UV Fe[b]		Small Blue Bump[c]			
						local cont.		global cont.	
ID	Object	Flux	EW	Flux	EW	Flux	EW	Flux	EW
1	MC2 0042+101	···	···	20^{+9}_{-9}	$40.0^{+61.1}_{-55.3}$	51	345	88	689
2	PG 0052+251	113^{+14}_{-14}	$52.6^{+7.8}_{-7.4}$	1144^{+249}_{-249}	$45.0^{+44.0}_{-41.3}$	2475	476	3727	817
3	PKS 0112−017	···	···	17^{+5}_{-5}	$83.0^{+23.9}_{-22.5}$	···	···	97	421
4	3C 37	11^{+3}_{-3}	$204.1^{+81.5}_{-70.0}$	43^{+15}_{-15}	$13.0^{+106.5}_{-90.2}$	69	442	98	690
5	3C 47	11^{+4}_{-4}	$67.1^{+30.5}_{-27.0}$	60^{+19}_{-19}	$15.0^{+49.6}_{-45.6}$	125	339	79	200
6	4C 01.04	34^{+11}_{-11}	$95.0^{+48.4}_{-38.2}$	57^{+36}_{-36}	$16.0^{+80.1}_{-70.5}$	208	516	171	409
7	4C 10.06	45^{+6}_{-6}	$59.9^{+8.3}_{-8.2}$	279^{+182}_{-182}	$18.0^{+96.0}_{-83.9}$	763	443	1013	640
8	PKS 0403−13	23^{+7}_{-7}	$67.1^{+19.4}_{-19.5}$	90^{+36}_{-36}	$84.0^{+56.8}_{-50.6}$	160	249	111	165
9	3C 110	11^{+32}_{-32}	$27.1^{+59.2}_{-88.4}$	163^{+50}_{-50}	$1.0^{+48.1}_{-44.4}$	468	491	729	926
10	3C 175	11^{+4}_{-4}	$21.1^{+8.4}_{-7.7}$	33^{+35}_{-35}	$2.0^{+24.2}_{-23.2}$	276	252	426	413
11	3C 186	···	···	33^{+11}_{-11}	$3.0^{+49.5}_{-45.6}$	52	246	100	527
12	B2 0742+31	34^{+10}_{-10}	$31.2^{+9.1}_{-9.0}$	549^{+82}_{-82}	$35.0^{+36.5}_{-34.7}$	1017	464	1992	1188
13	IRAS F07546+3928	1131^{+73}_{-73}	$188.7^{+21.3}_{-19.5}$	2101^{+661}_{-661}	$39.0^{+66.0}_{-57.1}$	3744	328	10846	1407
14	3C 207	11^{+2}_{-2}	$61.0^{+16.9}_{-14.7}$	37^{+23}_{-23}	$4.0^{+55.7}_{-50.5}$	144	390	255	813
15	PG 0844+349	1018^{+39}_{-39}	$211.8^{+11.0}_{-10.7}$	1503^{+698}_{-698}	$46.0^{+60.0}_{-53.5}$	4241	394	5214	505
16	PKS 0859−14	$23^{+1.}_{-1.}$	$94.1^{+0.6}_{-0.6}$	27^{+9}_{-9}	$85.0^{+19.3}_{-18.5}$	10	21	137	349
17	3C 215	11^{+6}_{-6}	$55.1^{+29.4}_{-29.1}$	17^{+20}_{-20}	$5.0^{+60.2}_{-53.5}$	72	222	91	295
18	4C 39.25	11^{+4}_{-4}	$22.0^{+9.7}_{-8.8}$	96^{+22}_{-22}	$27.0^{+17.7}_{-17.1}$	298	278	310	290
19	4C 40.24	···	···	17^{+4}_{-4}	$28.0^{+39.8}_{-36.7}$	26	237	31	297
20	PG 0947+396	113^{+31}_{-31}	$129.4^{+29.6}_{-31.8}$	485^{+142}_{-142}	$47.0^{+66.6}_{-59.5}$	1121	551	1337	694
21	PG 0953+414	113^{+28}_{-28}	$43.0^{+9.5}_{-9.9}$	618^{+364}_{-364}	$48.0^{+45.2}_{-41.8}$	1849	286	3379	594
22	4C 55.17	···	···	20^{+6}_{-6}	$31.0^{+26.0}_{-24.6}$	14	53	1	3
23	3C 232	45^{+9}_{-9}	$66.9^{+14.5}_{-14.3}$	233^{+30}_{-30}	$6.0^{+18.7}_{-18.1}$	363	246	1005	859
24	PG 1001+054	136^{+4}_{-4}	$202.7^{+10.9}_{-10.5}$	196^{+86}_{-86}	$49.0^{+57.2}_{-50.8}$	604	433	946	777
25	4C 22.26	···	···	20^{+6}_{-6}	$23.0^{+41.7}_{-39.0}$	42	297	45	327
26	4C 41.21	23^{+8}_{-8}	$61.8^{+20.5}_{-21.6}$	163^{+81}_{-81}	$29.0^{+71.5}_{-64.1}$	475	471	491	490
27	4C 20.24	···	···	63^{+16}_{-16}	$22.0^{+54.1}_{-50.5}$	82	271	114	393
28	PG 1100+772	79^{+54}_{-54}	$54.8^{+39.9}_{-37.8}$	339^{+199}_{-199}	$50.0^{+51.8}_{-47.7}$	487	136	1618	534
29	PG 1103−006	45^{+6}_{-6}	$98.0^{+17.3}_{-15.9}$	200^{+86}_{-86}	$51.0^{+66.2}_{-60.3}$	571	550	779	814
30	3C 254	11^{+15}_{-15}	$102.8^{+79.5}_{-150.2}$	53^{+16}_{-16}	$7.0^{+67.4}_{-60.3}$	128	561	153	708
31	PG 1114+445	102^{+10}_{-10}	$48.7^{+5.3}_{-5.2}$	768^{+235}_{-235}	$52.0^{+59.8}_{-54.9}$	1825	481	3669	1295
32	PG 1115+407	170^{+18}_{-18}	$150.0^{+28.1}_{-24.5}$	339^{+390}_{-390}	$53.0^{+123.0}_{-98.5}$	1029	358	1178	413
33	PG 1116+215	464^{+19}_{-19}	$171.7^{+11.3}_{-10.7}$	1892^{+296}_{-296}	$54.0^{+36.1}_{-34.2}$	3716	496	5315	782
34	4C 12.40	11^{+3}_{-3}	$142.5^{+48.3}_{-43.7}$	30^{+21}_{-21}	$20.0^{+127.2}_{-102.3}$	73	443	113	790
35	PKS 1127−14	···	···	50^{+10}_{-10}	$86.0^{+24.4}_{-23.4}$	84	208	179	494
36	3C 263	45^{+11}_{-11}	$58.8^{+16.2}_{-15.6}$	206^{+77}_{-77}	$8.0^{+43.2}_{-40.7}$	457	284	404	247
37	MC2 1146+111	11^{+8}_{-8}	$111.3^{+105.2}_{-85.2}$	23^{+6}_{-6}	$41.0^{+24.4}_{-23.3}$	63	311	109	590
38	4C 49.22	45^{+6}_{-6}	$156.3^{+25.2}_{-23.8}$	183^{+61}_{-61}	$30.0^{+81.4}_{-72.8}$	381	538	356	484
39	TEX 1156+213	23^{+11}_{-11}	$58.4^{+28.0}_{-28.2}$	100^{+49}_{-49}	$89.0^{+47.1}_{-44.1}$	298	347	252	284
40	PG 1202+281	45^{+9}_{-9}	$59.8^{+14.3}_{-13.5}$	209^{+35}_{-35}	$55.0^{+21.0}_{-20.3}$	938	711	1254	1103
41	4C 64.15	···	···	10^{+4}_{-4}	$33.0^{+27.6}_{-25.9}$	11	69	64	512
42	PG 1216+069	57^{+13}_{-13}	$42.0^{+11.8}_{-10.9}$	432^{+80}_{-80}	$56.0^{+40.3}_{-37.5}$	260	99	825	358
43	PG 1226+023	2828^{+203}_{-203}	$111.5^{+10.3}_{-9.9}$	5347^{+3056}_{-3056}	$57.0^{+38.3}_{-35.6}$	16866	261	34656	609
44	4C 30.25	···	···	17^{+6}_{-6}	$24.0^{+90.7}_{-79.1}$	···	···	33	427
45	3C 277.1	23^{+9}_{-9}	$103.9^{+38.7}_{-39.0}$	106^{+38}_{-38}	$9.0^{+83.8}_{-72.5}$	242	492	185	353
46	PG 1259+593	339^{+40}_{-40}	$403.1^{+38.5}_{-40.1}$	352^{+206}_{-206}	$58.0^{+65.7}_{-59.7}$	502	175	1631	696
47	3C 281	11^{+9}_{-9}	$62.3^{+42.8}_{-46.9}$	60^{+24}_{-24}	$10.0^{+53.4}_{-48.9}$	115	279	217	587
48	PG 1309+355	147^{+9}_{-9}	$66.2^{+4.8}_{-4.7}$	585^{+168}_{-168}	$59.0^{+36.9}_{-34.9}$	1165	273	2001	518
49	PG 1322+659	113^{+12}_{-12}	$97.5^{+12.1}_{-11.7}$	336^{+262}_{-262}	$60.0^{+96.5}_{-81.0}$	1153	466	1294	543
50	3C 288.1	11^{+9}_{-9}	$121.7^{+129.0}_{-100.5}$	17^{+6}_{-6}	$11.0^{+23.2}_{-22.0}$	58	258	85	401
51	PG 1351+640	226^{+86}_{-86}	$29.3^{+12.5}_{-11.7}$	968^{+744}_{-744}	$61.0^{+93.7}_{-73.6}$	1035	94	3692	387
52	B2 1351+31	···	···	10^{+3}_{-3}	$36.0^{+26.4}_{-25.1}$	···	···	29	301
53	PG 1352+183	113^{+17}_{-17}	$112.5^{+20.9}_{-19.8}$	449^{+219}_{-219}	$62.0^{+77.6}_{-69.3}$	1153	471	1728	786
54	4C 19.44	34^{+12}_{-12}	$69.5^{+28.5}_{-26.7}$	196^{+58}_{-58}	$21.0^{+49.0}_{-45.8}$	338	304	727	794
55	4C 58.29	···	···	27^{+9}_{-9}	$32.0^{+21.2}_{-20.0}$	47	114	42	103
56	PG 1402+261	452^{+13}_{-13}	$259.5^{+15.5}_{-14.6}$	562^{+360}_{-360}	$63.0^{+60.1}_{-54.2}$	2059	436	3032	717
57	PG 1411+442	566^{+15}_{-15}	$122.9^{+3.1}_{-3.1}$	855^{+402}_{-402}	$64.0^{+36.9}_{-34.2}$	3398	363	5792	717
58	PG 1415+451	328^{+14}_{-14}	$210.3^{+14.5}_{-13.8}$	532^{+209}_{-209}	$65.0^{+65.1}_{-59.1}$	932	295	919	289
59	PG 1425+267	23^{+8}_{-8}	$34.4^{+13.9}_{-13.2}$	306^{+139}_{-139}	$66.0^{+93.9}_{-78.7}$	744	506	1132	889
60	PG 1427+480	57^{+4}_{-4}	$83.3^{+6.6}_{-6.5}$	236^{+59}_{-59}	$67.0^{+30.0}_{-28.6}$	734	443	931	593
61	PG 1440+356	1222^{+23}_{-23}	$230.1^{+8.6}_{-8.3}$	1383^{+738}_{-738}	$68.0^{+54.4}_{-49.2}$	3774	308	7478	719
62	PG 1444+407	328^{+6}_{-6}	$287.5^{+7.6}_{-7.4}$	226^{+80}_{-80}	$69.0^{+21.1}_{-20.3}$	1104	384	2213	960
63	PG 1512+370	11^{+11}_{-11}	$23.4^{+20.6}_{-21.7}$	193^{+52}_{-52}	$70.0^{+32.9}_{-31.3}$	688	572	994	976
64	PG 1534+580	57^{+72}_{-72}	$25.4^{+38.8}_{-31.7}$	898^{+434}_{-434}	$71.0^{+107.3}_{-88.1}$	1902	462	1159	252
65	PG 1543+489	136^{+11}_{-11}	$206.9^{+23.1}_{-21.9}$	190^{+28}_{-28}	$72.0^{+16.3}_{-15.6}$	256	152	1107	855

Table 5—Continued

		Optical Fe II[a]		UV Fe[b]		Small Blue Bump[c]			
						local cont.		global cont.	
ID	Object	Flux	EW	Flux	EW	Flux	EW	Flux	EW
66	PG 1545+210	23^{+8}_{-8}	$25.0^{+9.1}_{-8.7}$	419^{+138}_{-138}	$73.0^{+64.3}_{-58.1}$	1066	517	1397	748
67	B2 1555+33	...	...	17^{+7}_{-7}	$37.0^{+83.4}_{-71.0}$	32	346	42	471
68	B2 1611+34	...	...	30^{+7}_{-7}	$38.0^{+33.6}_{-30.9}$	8	31	12	49
69	3C 334	11^{+10}_{-10}	$26.2^{+24.8}_{-23.4}$	166^{+94}_{-94}	$12.0^{+80.6}_{-70.3}$	440	432	682	755
70	PG 1626+554	124^{+71}_{-71}	$72.2^{+61.7}_{-45.4}$	761^{+449}_{-449}	$74.0^{+101.9}_{-83.5}$	1794	410	2952	780
71	OS 562	23^{+53}_{-53}	$77.4^{+86.0}_{-321.4}$	80^{+25}_{-25}	$44.0^{+35.8}_{-33.7}$	138	215	232	389
72	PKS 1656+053	57^{+8}_{-8}	$114.1^{+19.5}_{-18.6}$	96^{+14}_{-14}	$87.0^{+15.4}_{-14.9}$	59	64	168	190
73	PG 1704+608	23^{+14}_{-14}	$13.6^{+8.6}_{-8.6}$	246^{+157}_{-157}	$75.0^{+47.0}_{-43.7}$	316	99	502	162
74	MRK 506	283^{+47}_{-47}	$101.5^{+18.7}_{-18.2}$	1496^{+140}_{-140}	$42.0^{+44.9}_{-42.8}$	1767	344	1551	300
75	4C 34.47	226^{+30}_{-30}	$167.2^{+31.2}_{-28.4}$	416^{+141}_{-141}	$26.0^{+34.2}_{-31.9}$	1712	497	2837	1007
76	4C 73.18	79^{+11}_{-11}	$41.2^{+6.2}_{-6.1}$	439^{+177}_{-177}	$34.0^{+34.1}_{-31.9}$	2201	554	1886	456
77	MRK 509	1142^{+149}_{-149}	$99.7^{+17.0}_{-15.8}$	5081^{+569}_{-569}	$43.0^{+18.1}_{-17.4}$	13105	469	23929	1043
78	4C 06.69	23^{+13}_{-13}	$42.1^{+25.5}_{-24.1}$	53^{+13}_{-13}	$17.0^{+11.0}_{-10.8}$	147	143	139	134
79	4C 31.63	283^{+18}_{-18}	$114.5^{+8.0}_{-8.0}$	791^{+554}_{-554}	$25.0^{+64.6}_{-56.4}$	2695	387	5399	943
80	PG 2214+139	1131^{+101}_{-101}	$173.3^{+27.8}_{-24.6}$	1736^{+1482}_{-1482}	$76.0^{+93.5}_{-73.6}$	6074	407	8492	624
81	PKS 2216−038	45^{+19}_{-19}	$82.0^{+40.2}_{-36.8}$	173^{+40}_{-40}	$88.0^{+42.7}_{-40.0}$	269	266	483	531
82	3C 446	...	...	17^{+9}_{-9}	$14.0^{+43.3}_{-39.3}$	...	...	53	213
83	4C 11.69	...	...	50^{+25}_{-25}	$19.0^{+34.3}_{-32.2}$	...	...	161	220
84	PG 2251+113	226^{+29}_{-29}	$145.0^{+26.7}_{-24.3}$	426^{+198}_{-198}	$77.0^{+56.0}_{-49.6}$	1411	453	2101	760
85	PG 2349−014	136^{+24}_{-24}	$106.6^{+31.1}_{-25.9}$	515^{+209}_{-209}	$78.0^{+73.4}_{-61.4}$	1334	493	1708	677

Note. — Same as Table 2 for UV and optical Fe emissions, and the Small Blue Bump.

[a]Flux is from the template fitting between 4478–5640Å. EW is calculated using the local continuum at 4861Å.

[b]Flux is from the template fitting between 2230–3016Å. EW is calculated using the local continuum at 2799Å.

[c]The small blue bump is not discussed in this paper. See Shang et al. (2007) for descriptions.

Table 6. Parameters of Strong Emission Lines Na I+He I and Hα

		Na I $\lambda\lambda$5890,5896 + He I λ5876				Hα				
ID	Object	Flux	EW	FWHM	Δv[a]	Flux	EW	FWHM	Δv	Asymm
1	MC2 0042+101	...	...	...	...	...	...	...	...	...
2	PG 0052+251	$49.3^{+9.0}_{-7.3}$	$28.5^{+5.6}_{-5.5}$	4745^{+345}_{-300}	−100	$759.3^{+6.9}_{-6.1}$	$446.5^{+9.4}_{-9.2}$	4465^{+10}_{-10}	−70	$0.000^{+0.001}_{-0.001}$
3	PKS 0112−017	...	...	...	...	...	...	...	...	...
4	3C 37	...	...	...	...	...	...	...	...	...
5	3C 47	$2.0^{+5.4}_{-3.6}$	$12.6^{+40.4}_{-31.4}$	6815^{+1175}_{-0}	45	$98.4^{+9.4}_{-7.4}$	$612.2^{+153.7}_{-119.7}$	5125^{+295}_{-255}	−100	$0.000^{+0.101}_{-0.112}$
6	4C 01.04	...	...	...	...	$120.0^{+9.4}_{-7.4}$	$301.4^{+40.8}_{-36.9}$	8335^{+130}_{-130}	2075	$0.000^{+0.013}_{-0.012}$
7	4C 10.06	$9.0^{+5.5}_{-3.7}$	$13.7^{+9.2}_{-8.6}$	4560^{+1050}_{-810}	190	$335.6^{+21.1}_{-17.6}$	$507.8^{+66.6}_{-59.0}$	4720^{+60}_{-55}	260	$-0.056^{+0.009}_{-0.011}$
8	PKS 0403−13	...	...	...	...	$86.1^{+1.0}_{-0.9}$	$316.9^{+3.6}_{-3.6}$	3320^{+5}_{-10}	220	$-0.139^{+0.002}_{-0.001}$
9	3C 110	4.0	15.6	6815	45	$83.8^{+2.3}_{-2.0}$	$384.5^{+10.6}_{-10.6}$	7030^{+45}_{-50}	−250	$-0.049^{+0.006}_{-0.006}$
10	3C 175	...	...	...	...	$172.4^{+8.5}_{-7.3}$	$480.5^{+38.1}_{-36.0}$	13845^{+175}_{-175}	190	$0.053^{+0.016}_{-0.018}$
11	3C 186	...	...	...	...	...	...	...	...	...
12	B2 0742+31	$15.0^{+8.5}_{-6.5}$	$17.9^{+11.1}_{-10.4}$	6815^{+460}_{-0}	45	$458.9^{+28.3}_{-24.0}$	$576.5^{+76.6}_{-67.5}$	5885^{+90}_{-85}	−120	$0.000^{+0.012}_{-0.013}$
13	IRAS F07546	$73.5^{+29.5}_{-21.5}$	$14.8^{+6.2}_{-6.0}$	2220^{+185}_{-160}	65	$1906.4^{+25.0}_{-21.8}$	$396.4^{+10.3}_{-10.0}$	1990^{+10}_{-0}	125	$0.000^{+0.000}_{-0.001}$
14	3C 207	...	...	...	...	$37.5^{+0.6}_{-0.6}$	$286.9^{+4.8}_{-4.8}$	3245^{+10}_{-20}	20	$0.000^{+0.001}_{-0.001}$
15	PG 0844+349	$45.7^{+18.8}_{-13.5}$	$10.3^{+4.4}_{-4.3}$	2465^{+190}_{-175}	70	$1068.7^{+21.0}_{-18.1}$	$253.5^{+7.5}_{-7.3}$	2325^{+0}_{-0}	325	$0.000^{+0.000}_{-0.000}$
16	PKS 0859−14	...	...	...	...	...	...	...	...	...
17	3C 215	...	...	...	...	$44.8^{+3.9}_{-3.3}$	$259.7^{+39.7}_{-35.4}$	6155^{+145}_{-140}	190	$0.000^{+0.009}_{-0.010}$
18	4C 39.25	...	...	...	...	$107.4^{+0.7}_{-0.6}$	$379.2^{+2.3}_{-2.3}$	4515^{+0}_{-10}	860	$0.000^{+0.001}_{-0.001}$
19	4C 40.24	...	...	...	...	...	...	...	...	...
20	PG 0947+396	$22.8^{+9.9}_{-7.4}$	$30.8^{+15.3}_{-14.1}$	5740^{+935}_{-840}	170	$393.0^{+21.1}_{-17.8}$	$504.5^{+63.6}_{-55.9}$	3805^{+40}_{-40}	−25	$0.000^{+0.005}_{-0.005}$
21	PG 0953+414	$22.8^{+13.0}_{-7.7}$	$12.3^{+7.4}_{-7.1}$	2905^{+325}_{-305}	510	$501.6^{+20.7}_{-17.0}$	$284.6^{+20.4}_{-19.3}$	3175^{+20}_{-20}	80	$-0.001^{+0.002}_{-0.002}$
22	4C 55.17	...	...	...	...	...	...	...	...	...
23	3C 232	$8.0^{+5.4}_{-3.6}$	$13.3^{+9.7}_{-9.0}$	4630^{+1175}_{-955}	45	$93.0^{+12.2}_{-9.7}$	$167.4^{+32.7}_{-29.3}$	2105^{+35}_{-45}	−245	$0.000^{+0.007}_{-0.006}$
24	PG 1001+054	$8.4^{+1.7}_{-1.3}$	$17.0^{+3.9}_{-3.7}$	3010^{+185}_{-160}	300	$199.7^{+1.9}_{-1.7}$	$457.7^{+15.2}_{-14.5}$	1730^{+0}_{-0}	80	$0.075^{+0.001}_{-0.002}$
25	4C 22.26	...	...	...	...	...	...	...	...	...
26	4C 41.21	$6.0^{+13.6}_{-10.2}$	$17.9^{+46.0}_{-38.5}$	6815^{+730}_{-0}	45	$142.7^{+1.6}_{-1.4}$	$487.6^{+5.5}_{-5.5}$	3290^{+10}_{-5}	−160	$0.134^{+0.002}_{-0.003}$
27	4C 20.24	...	...	...	...	...	...	...	...	...
28	PG 1100+772	$6.9^{+7.3}_{-4.2}$	$6.2^{+7.1}_{-6.6}$	3530^{+2175}_{-1395}	480	$482.4^{+18.4}_{-16.0}$	$485.9^{+34.2}_{-32.2}$	6910^{+80}_{-70}	20	$0.000^{+0.008}_{-0.009}$
29	PG 1103−006	$7.1^{+2.1}_{-1.6}$	$19.5^{+6.4}_{-6.1}$	6620^{+635}_{-605}	100	$103.1^{+7.0}_{-5.9}$	$332.6^{+34.5}_{-32.3}$	5165^{+65}_{-65}	5	$0.000^{+0.009}_{-0.009}$
30	3C 254	...	...	...	...	...	...	...	...	...
31	PG 1114+445	$36.7^{+10.8}_{-8.4}$	$22.6^{+7.0}_{-6.8}$	5310^{+730}_{-585}	355	$720.6^{+12.3}_{-10.8}$	$485.7^{+15.0}_{-14.6}$	3955^{+15}_{-10}	150	$-0.024^{+0.003}_{-0.002}$
32	PG 1115+407	$17.2^{+2.1}_{-1.7}$	$17.5^{+2.4}_{-2.3}$	2300^{+40}_{-50}	505	$317.8^{+3.2}_{-2.8}$	$355.4^{+7.6}_{-7.4}$	1690^{+0}_{-0}	260	$-0.006^{+0.000}_{-0.001}$
33	PG 1116+215	$47.7^{+4.3}_{-3.5}$	$23.6^{+2.3}_{-2.3}$	3535^{+65}_{-65}	180	$1153.2^{+11.4}_{-10.1}$	$646.6^{+13.8}_{-13.5}$	2720^{+0}_{-0}	235	$0.019^{+0.001}_{-0.001}$
34	4C 12.40	...	...	...	...	...	...	...	...	...
35	PKS 1127−14	...	...	...	...	...	...	...	...	...
36	3C 263	...	...	...	...	...	...	...	...	...
37	MC2 1146+111	...	...	...	...	...	...	...	...	...
38	4C 49.22	$6.7^{+2.9}_{-2.0}$	$23.9^{+11.6}_{-10.8}$	3945^{+455}_{-410}	435	$133.1^{+13.9}_{-11.2}$	$468.0^{+109.9}_{-88.9}$	3555^{+65}_{-60}	320	$0.000^{+0.008}_{-0.009}$
39	TEX 1156+213	$2.0^{+2.6}_{-1.9}$	$6.3^{+8.1}_{-8.1}$	6815^{+65}_{-0}	45	$171.6^{+19.8}_{-16.2}$	$517.7^{+117.3}_{-97.8}$	6895^{+185}_{-180}	−535	$0.000^{+0.024}_{-0.027}$
40	PG 1202+281	$18.1^{+4.6}_{-3.7}$	$28.6^{+7.9}_{-7.6}$	3795^{+1150}_{-1280}	35	$334.9^{+4.1}_{-3.6}$	$559.1^{+16.4}_{-15.9}$	4015^{+10}_{-5}	−300	$-0.035^{+0.000}_{-0.002}$
41	4C 64.15	...	...	...	...	...	...	...	...	...
42	PG 1216+069	$10.5^{+8.0}_{-5.3}$	$10.5^{+8.4}_{-8.0}$	3965^{+2320}_{-1305}	145	$344.9^{+11.5}_{-9.9}$	$375.9^{+21.2}_{-20.3}$	4350^{+30}_{-25}	270	$0.039^{+0.004}_{-0.004}$
43	PG 1226+023	$140.5^{+21.8}_{-18.0}$	$7.8^{+1.3}_{-1.2}$	3555^{+160}_{-155}	455	$4501.8^{+62.0}_{-54.6}$	$280.5^{+5.8}_{-5.8}$	3115^{+0}_{-10}	65	$-0.001^{+0.001}_{-0.001}$
44	4C 30.25	...	...	...	...	...	...	...	...	...
45	3C 277.1	$4.0^{+5.4}_{-3.6}$	$19.9^{+31.9}_{-26.1}$	6815^{+1175}_{-0}	45	$85.0^{+9.4}_{-7.4}$	$470.1^{+116.9}_{-93.6}$	3210^{+50}_{-60}	65	$0.000^{+0.005}_{-0.005}$

Table 6—Continued

ID	Object	Na I λλ5890,5896 + He I λ5876 Flux	EW	FWHM	Δv[a]	Hα Flux	EW	FWHM	Δv	Asymm
46	PG 1259+593	···	···	···	···	$220.0^{+45.3}_{-35.4}$	$303.3^{+120.9}_{-91.6}$	2575^{+100}_{-100}	5	$-0.001^{+0.038}_{-0.041}$
47	3C 281	···	···	···	···	···	···	···	···	···
48	PG 1309+355	$23.2^{+6.9}_{-5.0}$	$13.2^{+4.0}_{-4.0}$	3950^{+165}_{-160}	445	$415.5^{+9.7}_{-8.4}$	$263.4^{+9.6}_{-9.4}$	3010^{+10}_{-10}	345	$-0.066^{+0.002}_{-0.003}$
49	PG 1322+659	$14.6^{+5.4}_{-3.9}$	$16.9^{+6.8}_{-6.5}$	3815^{+365}_{-345}	60	$248.2^{+23.8}_{-18.8}$	$287.8^{+51.2}_{-44.6}$	2860^{+40}_{-45}	170	$-0.001^{+0.004}_{-0.004}$
50	3C 288.1	···	···	···	···	···	···	···	···	···
51	PG 1351+640	$76.9^{+20.2}_{-15.8}$	$12.3^{+3.4}_{-3.3}$	1905^{+115}_{-105}	−5	$1059.8^{+26.5}_{-23.2}$	$185.7^{+6.3}_{-6.2}$	2305^{+10}_{-10}	45	$0.000^{+0.005}_{-0.005}$
52	B2 1351+31	···	···	···	···	···	···	···	···	···
53	PG 1352+183	$18.1^{+7.8}_{-5.4}$	$24.0^{+11.3}_{-10.7}$	4505^{+440}_{-400}	10	$289.4^{+13.5}_{-11.3}$	$434.3^{+41.7}_{-38.1}$	3600^{+25}_{-30}	215	$0.012^{+0.002}_{-0.003}$
54	4C 19.44	···	···	···	···	···	···	···	···	···
55	4C 58.29	···	···	···	···	···	···	···	···	···
56	PG 1402+261	$29.1^{+4.4}_{-3.4}$	$22.3^{+3.8}_{-3.7}$	2320^{+55}_{-55}	520	$520.9^{+1.3}_{-1.2}$	$444.8^{+1.1}_{-1.1}$	1885^{+0}_{-0}	125	$0.003^{+0.000}_{-0.000}$
57	PG 1411+442	$32.7^{+5.2}_{-4.2}$	$9.5^{+1.6}_{-1.6}$	2190^{+90}_{-80}	10	$1371.9^{+8.1}_{-7.3}$	$441.5^{+5.5}_{-5.4}$	2185^{+0}_{-0}	−105	$-0.027^{+0.001}_{-0.000}$
58	PG 1415+451	$15.8^{+2.8}_{-2.3}$	$11.4^{+2.2}_{-2.1}$	2575^{+125}_{-115}	145	$327.9^{+3.1}_{-2.8}$	$254.9^{+4.4}_{-4.4}$	1965^{+5}_{-0}	80	$0.039^{+0.002}_{-0.000}$
59	PG 1425+267	$5.8^{+3.6}_{-2.5}$	$11.6^{+7.5}_{-7.2}$	5800^{+1500}_{-1210}	−1090	$223.2^{+14.4}_{-12.3}$	$496.3^{+56.6}_{-51.8}$	8670^{+150}_{-150}	420	$0.042^{+0.016}_{-0.017}$
60	PG 1427+480	$9.9^{+2.1}_{-1.6}$	$19.4^{+4.5}_{-4.3}$	2540^{+100}_{-85}	425	$183.1^{+3.4}_{-3.0}$	$405.4^{+16.9}_{-16.2}$	2000^{+10}_{-0}	210	$-0.030^{+0.003}_{-0.002}$
61	PG 1440+356	$36.3^{+2.9}_{-2.3}$	$8.3^{+0.7}_{-0.7}$	1980^{+40}_{-30}	190	$1023.8^{+6.0}_{-5.4}$	$247.6^{+2.7}_{-2.6}$	1125^{+0}_{-5}	−35	$0.013^{+0.002}_{-0.000}$
62	PG 1444+407	$17.9^{+5.6}_{-4.0}$	$21.7^{+7.1}_{-6.9}$	2710^{+135}_{-125}	660	$314.7^{+8.5}_{-7.3}$	$447.7^{+18.7}_{-18.2}$	2520^{+10}_{-5}	145	$0.002^{+0.001}_{-0.001}$
63	PG 1512+370	···	···	···	···	$163.6^{+21.7}_{-18.0}$	$503.2^{+146.8}_{-114.6}$	6235^{+280}_{-275}	270	$0.099^{+0.028}_{-0.029}$
64	PG 1534+580	$65.6^{+27.1}_{-20.5}$	$32.0^{+14.9}_{-13.9}$	6765^{+995}_{-925}	−225	$553.2^{+24.6}_{-21.4}$	$286.5^{+24.0}_{-22.3}$	4840^{+60}_{-55}	−315	$0.014^{+0.005}_{-0.004}$
65	PG 1543+489	$8.1^{+6.8}_{-3.9}$	$18.0^{+16.0}_{-15.3}$	2425^{+325}_{-285}	480	$162.5^{+2.5}_{-2.2}$	$352.7^{+13.3}_{-12.7}$	1485^{+0}_{-5}	240	$0.044^{+0.001}_{-0.002}$
66	PG 1545+210	$9.0^{+4.6}_{-3.3}$	$12.9^{+7.1}_{-6.7}$	4805^{+995}_{-770}	45	$421.0^{+9.5}_{-8.3}$	$650.9^{+25.2}_{-24.4}$	5950^{+25}_{-20}	480	$0.000^{+0.003}_{-0.002}$
67	B2 1555+33	···	···	···	···	···	···	···	···	···
68	B2 1611+34	···	···	···	···	$13.5^{+0.4}_{-0.4}$	$152.1^{+4.5}_{-4.5}$	2740^{+20}_{-15}	590	$-0.114^{+0.008}_{-0.007}$
69	3C 334	···	···	···	···	···	···	···	···	···
70	PG 1626+554	$31.5^{+25.6}_{-15.4}$	$26.1^{+24.1}_{-21.5}$	4890^{+1305}_{-1055}	430	$548.9^{+46.2}_{-37.5}$	$528.1^{+98.7}_{-82.9}$	3835^{+55}_{-55}	140	$-0.038^{+0.007}_{-0.007}$
71	OS 562	···	···	···	···	···	···	···	···	···
72	PKS 1656+053	···	···	···	···	···	···	···	···	···
73	PG 1704+608	···	···	···	···	···	···	···	···	···
74	MRK 506	$64.8^{+10.3}_{-8.4}$	$26.9^{+4.5}_{-4.5}$	6380^{+330}_{-300}	−480	$779.7^{+31.8}_{-26.8}$	$344.5^{+22.1}_{-21.2}$	3770^{+20}_{-20}	−110	$0.013^{+0.002}_{-0.003}$
75	4C 34.47	$37.4^{+13.6}_{-10.2}$	$32.4^{+12.9}_{-12.3}$	4815^{+730}_{-590}	−5	$624.4^{+38.6}_{-32.4}$	$536.3^{+69.6}_{-61.7}$	2820^{+25}_{-20}	−175	$-0.042^{+0.004}_{-0.003}$
76	4C 73.18	$29.1^{+8.5}_{-6.5}$	$18.3^{+5.8}_{-5.6}$	4710^{+460}_{-410}	−15	$688.9^{+14.0}_{-12.3}$	$466.0^{+19.3}_{-18.6}$	2750^{+10}_{-5}	−60	$-0.001^{+0.002}_{-0.002}$
77	MRK 509	$307.7^{+64.5}_{-50.7}$	$33.3^{+7.6}_{-7.4}$	2805^{+120}_{-115}	75	$4985.1^{+81.6}_{-69.6}$	$552.6^{+18.6}_{-17.9}$	3335^{+5}_{-10}	20	$0.013^{+0.001}_{-0.000}$
78	4C 06.69	···	···	···	···	···	···	···	···	···
79	4C 31.63	···	···	···	···	···	···	···	···	···
80	PG 2214+139	$99.8^{+24.0}_{-18.6}$	$17.8^{+4.5}_{-4.4}$	4570^{+295}_{-265}	−145	$1555.5^{+16.0}_{-14.3}$	$280.4^{+4.9}_{-4.9}$	5150^{+15}_{-10}	20	$0.000^{+0.001}_{-0.001}$
81	PKS 2216−038	···	···	···	···	···	···	···	···	···
82	3C 446	···	···	···	···	···	···	···	···	···
83	4C 11.69	···	···	···	···	···	···	···	···	···
84	PG 2251+113	$20.0^{+15.4}_{-10.3}$	$16.9^{+14.3}_{-13.2}$	5800^{+1865}_{-1535}	45	$726.3^{+32.7}_{-28.0}$	$673.8^{+64.6}_{-58.8}$	4650^{+40}_{-40}	−505	$0.000^{+0.010}_{-0.011}$
85	PG 2349−014	$28.2^{+4.1}_{-3.4}$	$27.0^{+4.2}_{-4.1}$	7930^{+375}_{-355}	20	$404.7^{+8.6}_{-7.6}$	$343.4^{+13.4}_{-12.9}$	4800^{+25}_{-25}	0	$0.000^{+0.003}_{-0.003}$

Note. — Same as Table 2 for Na I+He I and Hα emission lines.

[a]Calculated using He I λ5876 wavelength.

Table 7. Measured FWHM and Flux Density

ID	Object	FWHM (km s^{-1}) Mg II	Hβ	C IV	f_{1350}[a]	f_{3000}[a]	f_{5100}[a]
1	MC2 0042+101	6275	8270	4195	0.32	0.16	0.08
2	PG 0052+251	4510	6460	5815	18.96	6.06	1.99
3	PKS 0112−017	4130	···	5030	0.75	0.21	0.09
4	3C 37	4200	4280	3360	0.44	0.18	0.05
5	3C 47	7745	14005	5450	1.57	0.41	0.16
6	4C 01.04	9550	9905	6665	0.74	0.53	0.35
7	4C 10.06	4670	4735	3785	6.60	2.04	0.70
8	PKS 0403−13	3535	3735	3325	1.77	0.71	0.32
9	3C 110	5645	12450	5700	4.14	1.12	0.38
10	3C 175	9515	20925	6915	3.41	1.37	0.52
11	3C 186	5790	···	6290	0.69	0.22	0.10
12	B2 0742+31	6060	10690	4890	4.95	2.59	1.00
13	IRAS F07546+3928	2045	2785	3035	16.01	12.91	5.66
14	3C 207	4140	3505	4935	0.95	0.43	0.17
15	PG 0844+349	3160	2870	4550	31.30	13.00	4.50
16	PKS 0859−14	3775	4615	4520	1.48	0.47	0.22
17	3C 215	6260	6760	5605	0.99	0.34	0.20
18	4C 39.25	5075	6400	4775	3.69	1.23	0.51
19	4C 40.24	3650	···	4920	0.33	0.11	0.05
20	PG 0947+396	4170	4340	3925	7.09	2.60	0.82
21	PG 0953+414	2700	2990	3810	28.25	8.27	2.36
22	4C 55.17	3475	···	6420	0.66	0.25	0.13
23	3C 232	4620	4655	7145	3.11	1.70	0.61
24	PG 1001+054	2280	2615	3130	4.10	1.68	0.61
25	4C 22.26	4910	···	5015	0.53	0.16	0.07
26	4C 41.21	3060	3445	3800	5.62	1.18	0.34
27	4C 20.24	4070	···	3525	0.85	0.30	0.12
28	PG 1100+772	6090	9390	4775	14.66	3.76	1.31
29	PG 1103−006	4780	5270	4515	3.77	1.37	0.43
30	3C 254	6595	14095	5205	0.76	0.27	0.11
31	PG 1114+445	4255	4825	3935	6.07	4.54	1.93
32	PG 1115+407	2750	1895	4585	12.93	3.47	1.06
33	PG 1116+215	2885	2975	3865	36.21	8.60	2.42
34	4C 12.40	4205	3565	5300	0.74	0.19	0.08
35	PKS 1127−14	3725	···	3695	1.33	0.43	0.18
36	3C 263	4265	4970	3310	5.61	1.83	0.68
37	MC2 1146+111	5020	7835	3715	0.48	0.23	0.10
38	4C 49.22	4415	3910	4535	2.44	0.82	0.28
39	TEX 1156+213	5175	7740	3880	3.15	1.04	0.36
40	PG 1202+281	3990	4950	2945	2.43	1.90	0.70
41	4C 64.15	5125	···	7245	0.45	0.15	0.08
42	PG 1216+069	3085	5950	3105	6.13	2.17	1.23
43	PG 1226+023	2935	3405	4530	269.97	76.67	23.06
44	4C 30.25	4440	···	3730	0.26	0.07	0.02
45	3C 277.1	3380	3835	3215	1.92	0.53	0.21

Table 7—Continued

ID	Object	FWHM (km s^{-1}) Mg II	Hβ	C IV	f_{1350}[a]	f_{3000}[a]	f_{5100}[a]
46	PG 1259+593	3650	4035	6880	10.83	3.13	0.75
47	3C 281	5505	7985	4865	1.51	0.46	0.17
48	PG 1309+355	3355	3640	2815	10.56	4.71	2.08
49	PG 1322+659	2765	3285	3690	9.60	3.01	1.06
50	3C 288.1	4320	8970	4015	0.81	0.26	0.09
51	PG 1351+640	1400	6205	4050	16.65	9.65	7.35
52	B2 1351+31	4205	···	3690	0.35	0.11	0.05
53	PG 1352+183	4175	4210	3755	9.47	2.98	0.91
54	4C 19.44	3105	4575	2730	3.69	1.21	0.48
55	4C 58.29	4830	···	5745	1.53	0.42	0.19
56	PG 1402+261	2460	2100	4550	21.81	6.12	1.54
57	PG 1411+442	1975	2800	2040	25.60	11.77	4.20
58	PG 1415+451	2425	2560	3725	9.59	3.45	1.48
59	PG 1425+267	8280	9875	7060	4.15	1.81	0.60
60	PG 1427+480	2415	2405	2835	7.07	2.00	0.62
61	PG 1440+356	1800	1745	2130	43.44	14.18	4.93
62	PG 1444+407	2760	2750	4425	9.31	3.85	1.02
63	PG 1512+370	6545	7690	3970	4.18	1.75	0.43
64	PG 1534+580	3305	4505	3790	14.03	5.02	2.12
65	PG 1543+489	1980	2320	5625	5.72	1.87	0.59
66	PG 1545+210	5230	6885	4560	6.65	2.35	0.85
67	B2 1555+33	4650	···	4240	0.32	0.10	0.06
68	B2 1611+34	4010	4795	4625	0.85	0.23	0.13
69	3C 334	4840	6345	5745	3.84	1.27	0.39
70	PG 1626+554	4155	4390	3815	16.51	5.18	1.55
71	OS 562	3465	3305	3470	2.71	0.70	0.29
72	PKS 1656+053	3980	3510	···	2.67	0.93	0.48
73	PG 1704+608	8405	10465	4015	8.92	3.28	1.56
74	MRK 506	5130	4840	5290	12.55	3.55	2.58
75	4C 34.47	3175	5015	2855	9.19	4.60	1.25
76	4C 73.18	3345	3095	3560	13.00	5.61	1.80
77	MRK 509	3680	3825	4710	84.93	33.87	10.62
78	4C 06.69	4220	4015	5620	3.84	1.10	0.51
79	4C 31.63	4055	3395	4840	34.43	9.10	2.20
80	PG 2214+139	6220	5845	2690	46.53	19.66	6.08
81	PKS 2216−038	3555	4415	3600	2.35	1.01	0.52
82	3C 446	3955	···	3390	0.38	0.24	0.18
83	4C 11.69	3675	···	3185	2.10	0.74	0.40
84	PG 2251+113	4110	4060	4805	8.80	4.03	1.45
85	PG 2349−014	4825	6325	5675	9.48	3.60	1.18

[a]Observed-frame flux density at rest-frame 1350, 3000, and 5100 Å in the units of 10^{-15}erg s^{-1} cm^{-2} Å^{-1}, from fitted local continuum in each region.

Table 8. Luminosity, Black Hole Mass, and Eddington Ratio

ID	Object	log $M_{\rm BH}$ ($M_\odot$) Mg II	Hβ	C IV	Adopted[a]	$\log(L_{Bol})$[b]	L/L_{Edd}	L_{Bol} Note[c]
1	MC2 0042+101	8.97	9.21	8.43	8.97	45.68	0.04	calc
2	PG 0052+251	8.74	8.97	8.87	8.87	45.94	0.09	
3	PKS 0112−017	9.21	···	9.36	9.29	46.88	0.31	
4	3C 37	8.72	8.62	8.39	8.62	46.18	0.29	
5	3C 47	9.17	9.64	8.82	9.17	45.97	0.05	
6	4C 01.04	9.14	9.25	8.54	9.14	45.44	0.02	
7	4C 10.06	9.05	9.00	8.81	9.00	46.48	0.24	
8	PKS 0403−13	8.78	8.82	8.60	8.78	46.36	0.30	
9	3C 110	9.47	10.09	9.47	9.47	46.99	0.26	calc
10	3C 175	9.97	10.60	9.58	9.97	46.91	0.07	calc
11	3C 186	9.35	···	9.35	9.35	46.66	0.16	calc
12	B2 0742+31	9.40	9.85	9.04	9.40	46.46	0.09	
13	IRAS F07546+3928	7.97	8.23	8.01	8.01	45.43	0.21	
14	3C 207	8.92	8.74	8.92	8.92	46.28	0.19	calc
15	PG 0844+349	8.17	8.02	8.32	8.17	45.31	0.11	
16	PKS 0859−14	9.29	9.46	9.40	9.40	47.22	0.53	calc
17	3C 215	8.92	9.04	8.72	8.92	45.77	0.06	
18	4C 39.25	9.33	9.51	9.21	9.33	46.91	0.30	
19	4C 40.24	8.90	···	9.08	9.00	46.60	0.31	
20	PG 0947+396	8.63	8.58	8.46	8.58	45.80	0.13	
21	PG 0953+414	8.57	8.55	8.82	8.57	46.42	0.56	
22	4C 55.17	8.82	···	9.25	9.09	46.46	0.19	
23	3C 232	9.16	9.11	9.35	9.16	46.36	0.13	
24	PG 1001+054	7.88	7.95	8.00	7.95	45.13	0.12	
25	4C 22.26	9.07	···	9.04	9.05	46.59	0.28	
26	4C 41.21	8.81	8.80	9.03	8.81	46.75	0.70	
27	4C 20.24	9.14	···	8.93	9.05	46.92	0.59	
28	PG 1100+772	9.26	9.57	9.03	9.26	46.46	0.12	
29	PG 1103−006	9.01	9.00	8.85	9.00	46.30	0.16	calc
30	3C 254	9.27	9.89	8.96	9.27	46.17	0.06	
31	PG 1114+445	8.59	8.68	8.23	8.59	45.39	0.05	
32	PG 1115+407	8.18	7.77	8.57	8.18	45.72	0.27	
33	PG 1116+215	8.49	8.41	8.73	8.49	46.31	0.53	
34	4C 12.40	8.76	8.58	8.92	8.76	46.17	0.20	calc
35	PKS 1127−14	9.18	···	9.12	9.15	47.15	0.79	
36	3C 263	9.22	9.31	8.94	9.22	46.81	0.31	
37	MC2 1146+111	9.10	9.46	8.67	9.10	46.29	0.12	calc
38	4C 49.22	8.69	8.51	8.61	8.61	45.99	0.19	
39	TEX 1156+213	8.91	9.19	8.56	8.91	46.01	0.10	calc
40	PG 1202+281	8.41	8.55	7.84	8.41	45.41	0.08	
41	4C 64.15	9.29	···	9.52	9.42	46.73	0.16	calc
42	PG 1216+069	8.59	9.20	8.49	8.59	46.31	0.42	
43	PG 1226+023	8.92	8.96	9.27	8.96	46.96	0.80	
44	4C 30.25	8.87	···	8.67	8.78	46.27	0.24	calc
45	3C 277.1	8.34	8.41	8.24	8.34	45.61	0.15	

Table 8—Continued

ID	Object	log $M_{\rm BH}$ ($M_\odot$) Mg II	Hβ	C IV	Adopted[a]	log(L_{Bol})[b]	L/L_{Edd}	L_{Bol} Note[c]
46	PG 1259+593	9.02	8.97	9.54	9.02	46.83	0.52	calc
47	3C 281	9.10	9.38	8.93	9.10	46.23	0.11	
48	PG 1309+355	8.51	8.57	8.19	8.51	45.74	0.14	
49	PG 1322+659	8.20	8.29	8.36	8.29	45.74	0.22	
50	3C 288.1	9.06	9.63	8.93	9.06	46.61	0.28	calc
51	PG 1351+640	7.55	8.94	8.23	8.23	45.31	0.09	
52	B2 1351+31	9.06	···	8.89	8.98	46.66	0.38	calc
53	PG 1352+183	8.50	8.42	8.32	8.42	45.61	0.12	
54	4C 19.44	8.92	9.23	8.75	8.92	46.91	0.77	
55	4C 58.29	9.50	···	9.64	9.57	47.20	0.33	
56	PG 1402+261	8.24	7.97	8.72	8.24	46.02	0.47	
57	PG 1411+442	7.89	8.14	7.74	7.89	45.33	0.22	
58	PG 1415+451	7.92	7.95	8.17	7.95	45.37	0.21	
59	PG 1425+267	9.46	9.54	9.17	9.46	46.05	0.03	
60	PG 1427+480	8.14	8.04	8.21	8.14	45.79	0.36	
61	PG 1440+356	7.78	7.69	7.83	7.78	45.64	0.57	
62	PG 1444+407	8.50	8.37	8.77	8.50	46.20	0.40	
63	PG 1512+370	9.26	9.26	8.68	9.26	46.22	0.07	
64	PG 1534+580	7.66	7.90	7.61	7.66	44.43	0.05	calc
65	PG 1543+489	8.28	8.33	9.11	8.33	46.30	0.74	
66	PG 1545+210	8.94	9.12	8.71	8.94	45.93	0.08	
67	B2 1555+33	8.91	···	8.75	8.84	46.21	0.19	calc
68	B2 1611+34	9.22	9.41	9.32	9.32	47.06	0.43	calc
69	3C 334	9.16	9.31	9.24	9.24	46.44	0.13	
70	PG 1626+554	8.55	8.50	8.39	8.50	45.68	0.12	
71	OS 562	8.93	8.86	8.92	8.92	46.74	0.53	
72	PKS 1656+053	9.22	9.13	···	9.18	47.06	0.60	
73	PG 1704+608	9.61	9.81	8.87	9.61	46.49	0.06	
74	MRK 506	8.12	8.16	8.04	8.12	44.67	0.03	calc
75	4C 34.47	8.52	8.80	8.24	8.52	46.08	0.29	
76	4C 73.18	8.81	8.66	8.73	8.73	46.40	0.37	
77	MRK 509	8.22	8.17	8.28	8.22	45.36	0.11	
78	4C 06.69	9.38	9.33	9.61	9.38	47.30	0.67	
79	4C 31.63	9.07	8.78	9.21	9.07	46.61	0.28	
80	PG 2214+139	8.86	8.71	7.97	8.71	45.55	0.05	calc
81	PKS 2216−038	9.14	9.35	9.04	9.14	46.95	0.51	calc
82	3C 446	9.21	···	8.87	9.08	47.01	0.69	
83	4C 11.69	9.20	···	9.00	9.11	47.04	0.67	
84	PG 2251+113	8.96	8.89	8.94	8.94	46.35	0.20	calc
85	PG 2349−014	8.74	8.90	8.75	8.75	45.77	0.08	

[a]The adopted $M_{\rm BH}$ is the median of 3 available estimates or the mean in case of only 2 estimates.

[b]From Runnoe et al. (2012a). L_{Bol} is in erg s^{-1}, calculated using the full radio-to-X-ray SEDs (63 objects) except for the ones noted in the last column (22 objects).

[c]Those marked with "calc" indicate that L_{Bol} is calculated using equation 5 because the SEDs of these 22 objects do not have adequate X-ray or mid-infrared coverage (Runnoe et al. 2012a).